FUNCTIONAL ROLE OF ASPARTATE-31 AND LEUCINE-32 IN *MYCOBACTERIUM AVIUM* DIHYDROFOLATE REDUCTASE

By

RONNIE A. BOCK

Bachelor of Science in Biology
Universität des Saarlandes
Saarbrücken, Germany
1990

Master of Science in Biology
Universität des Saarlandes
Saarbrücken, Germany
1996

Submitted to the Faculty of the
Graduate College of the
Oklahoma State University
in partial fulfillment of
the requirements for
the Degree of
DOCTOR OF PHILOSOPHY
May, 2006

FUNCTIONAL ROLE OF ASPARTATE-31 AND

LEUCINE-32 IN *MYCOBACTERIUM AVIUM*

DIHYDROFOLATE REDUCTASE

Dissertation Approved:

Dr. W. Barrow

Dissertation Adviser

Dr. J. Malayer

Dr. K. Clinkenbeard

Dr. R. Burnap

Dr. G. Emslie

Dean of the Graduate College

ACKNOWLEDGEMENTS

I would like to express my sincere gratitude and appreciation to my supervisor and mentor Dr. William Barrow for the opportunity to work with him and his lab and to share in and benefit from their experience. Dr. Barrow's advice and guidance enabled me to not only complete my doctoral program, but prepared me for a new world of science and research. I will always be thankful for his patience and support.

I am thankful to my other committee members Dr. J. Malayer, Dr. K. Clinkenbeard and Dr. R. Burnap for their advice and interest. Their time in reading through my proposal and this dissertation, their input and suggestions and critical questioning during our meetings is highly appreciated.

I would also like to acknowledge Esther Barrow, our lab manager, for creating the best working and learning atmosphere. Her patience and willingness to invest her time and energy in me, by sharing with me her knowledge, introducing me to everyone and by listening to me and answer all my questions, will forever be remembered. I am particularly grateful to her for showing such a genuine interest in my personal welfare and later that of my family. I am also thankful to our lab members Dr Michelle Valderas and Dr. Phil Bourne for all their valuable help and support during my entire program. Phil's help in preparing some of the graphic images in this dissertation and during other presentations is greatly appreciated

My thanks and appreciation also goes to Dr. Jose Soulages, Department of Biochemistry and Molecular Biology at OSU, for his help and support in all experiments and analysis

regarding circular dichroism. I am in debt to Ms Betty Handlin from CVHS at OSU for her ever friendly technical help in preparing this dissertation and her support and friendliness during my stay at OSU.

My research project was funded in part by NIH grant AI-41348 (PI Dr. William Barrow) and by the Sitlington Chair for Infectious Diseases, CVHS at OSU (Sitlington Professor Dr. William Barrow). My graduate studies and stay in the United States were funded by a scholarship from the Namibian Government, administered by the Africa-America-Institute (New York). I would also like to acknowledge the Staff Development Program of the University of Namibia, for granting me study leave for the duration of my doctoral program in the United States.

Last, but not least, my heartfelt appreciation and thanks goes to all my family, particularly my loving and supporting wife, Barbara and my dearest children Raoul, Lizle and Sharifa, for their love, support, understanding and all the sacrifices they had to endure during my studies. I dedicate this work to them all.

TABLE OF CONTENTS

CHAPTER I Introduction 1
Background 1
Objectives 11
Hypothesis 1 11
Hypothesis 2 15
Chapter 2 Materials and Methods 19
Bacterial strains used 19
Mycobacterium avium DHFR gene (*folA*) 19
Plasmid vector construct p807 for recombinant *M. avium* DHFR 19
Validation (Verification) of recombinant wild type *M. avium* DHFR 20
Transformation 20
Overnight cell growth 20
Plasmid DNA extraction 21
Determining plasmid DNA concentration and purity 22
Restriction endonuclease digestion and agarose gel electrophoresis 22
Sequencing 23
Pilot expression of recombinant wild type *M. avium* DHFR 23
Transformation 23
Growth and IPTG induction 23
BugBuster protein extraction 24
Polyacrylamide gel electrophoresis (SDS-PAGE) 25
Separating gels 25
Stacking gels 25
SDS sample buffer 26
Electrophoresis running buffer 26
Site-directed mutagenesis 26
Design and synthesis of mutagenic oligonucleotides 27
5'-Phosphorylation of mutagenic oligonucleotides 28
Mutagenesis reaction 28
Alkaline denaturation (dsDNA) 28
Agarose gel electrophoresis 29
Oligonucleotide hybridization 29
Mutant strand synthesis and ligation 31
Transformation of BMH 71-18 *mut*S (repair-minus strain) 32
Transformation and over night growth 32
Plasmid DNA extraction 32
Determination of plasmid DNA concentration and purity 32
Transformation of JM109 33
Transformation 33

Overnight cell growth 33
Plasmid DNA extraction 34
Determining plasmid DNA concentration and purity 34
Sequencing 34
Large scale protein expression of recombinant mutant DHFR 34
Transformation 34
Overnight cell growth and IPTG induction 34
BugBuster protein extraction 35
BioRAD protein determination (microassay procedure for microplates) 36
Polyacrylamide gel electrophoresis (SDS-PAGE) 37
Purification of recombinant mutant and wild type DHFR (semi-automated procedure) 37
His-Resin and column preparation (manual operation) 37
Loading and washing the column (manual operation) 38
Biologic LP chromatography system (BioRAD) 38
Elution (automated procedure) 39
Functionality of recombinant mutant DHFR 40
DHFR standard enzyme assay 40
Kinetic assay 41
IC_{50} determination 41
Growth complementation 43
Circular dichroism 46
CHAPTER III Results 48
Mutagenesis 48
Protein expression and purification 49
Aspartic acid 31 mutations 53
Specific activity 53
Kinetic characteristics of D31 mutant DHFR 56
Growth complementation 58
Leucine 32 mutations 61
Specific activity 61
Kinetic characteristics of L32 mutant DHFR 63
Growth complementation 65
Inhibitor IC_{50} assay 66
CHAPTER IV Discussion 71
Functionality of *M. avium* conserved aspartic acid 31 (D31) mutants 72
Functionality of *M. avium* conserved leucine 32 (L32) mutants 80
Chapter V Conclusion 89
REFERENCES 90

LIST OF TABLES

Table 1. IC_{50} for trimethoprim for DHFR of various organisms. 4
Table 2. Comparison of overall amino acid sequence identity in DHFR of various species. 6
Table 3.Mutations of D31 and their expected effects on functionality of *M. avium* DHFR 15
Table 4: Mutations of L32 and their expected effects on functionality of *M. avium* DHFR 18
Table 5. Restriction endonuclease reaction setup for excising the *folA* gene from the p807 plasmid construction 22
Table 6. *M. avium fol*A D31 and L32 mutants and primers used to construct them. 27
Table 7. Reaction set up for electro transformation of MG1655*folA::kan3* cells with plasmid DNA of the recombinant wild type and mutant *M. avium* DHFR. 44
Table 8. Semi-automated purification of recombinant wild type DHFR on His-Bind resin (Novagen) with a linear gradient of 5-500 mM imidazol 52
Table 9.Comparison of enzyme specific activity (µmole min^{-1} mg^{-1}) of D31 mutated (D31A, D31E, D31Q, D31N, D31L) and control mutant (V76A) DHFR to that of the recombinant wild type (p807) at pH 7.0 and 30°C using the ANOVA and Dunnett procedures in the SAS statistical software (SAS system for Windows V8, SAS Inst. Inc, NC, USA) Dunnett significance level $\alpha = 0.05$ 54
Table 10.Multiple comparison of enzyme specific activity (µmole min^{-1} mg^{-1}) of recombinant wild type (p807) and D31mutated (D31A, D31E, D31Q, D31N, D31L) as well as control (V76A) DHFR at pH 7.0 and 30°C using the ANOVA and TUKEY procedures in the SAS statistical software (SAS system for Windows V8, SAS Inst. Inc, NC, USA) . TUKEY significance level $\alpha = 0.05$. 55
Table 11:Kinetic parameters at pH 7.0 and 30°C of recombinant wild type and D31mutants of *M. avium* DHFR for FAH_2 and NADPH determined with the non-linear Michaelis-Menten curve fitting program Enzfitter (BioSoft, UK). 58
Table 12. Comparison of enzyme specific activity (µmole $min^{-1}mg^{-1}$) of L32 mutated (L32F, L32A, L32D) DHFR to that of the recombinant wild type (p807) at pH 7.0 and 30°C using the ANOVA and Dunnett procedures in the SAS statistical software (SAS)system for Windows V8, SAS Inst. Inc, NC, USA) Dunnett significance level $\alpha = 0.05$ 62
Table 13.Multiple comparison of enzyme specific activity (µmole $min^{-1}mg^{-1}$) of recombinant wild type (p807) and mutated (L32F, L32A, L32D) *M. avium* DHFR at pH 7.0 and 30°C using the ANOVA and TUKEY procedure in the

SAS statistical software (SAS system for Windows V8, SAS Inst. Inc, NC, USA). (TUKEY significance level alpha=0.05). 63
Table 14. Kinetic parameters at pH 7.0 and 30°C of recombinant wild type and L32 mutants of *M. avium* DHFR for FAH_2 and NADPH determined with the non-linear Michaelis-Menten curve fitting program Enzfitter (BioSoft, UK). 65
Table 15. IC_{50} of trimethoprim (TMP) and SRI compounds 8858 and 20730 for recombinant wild type and leucine 32 mutant *M. avium* DHFR as determined by the 4 parameter curve procedure (the Bio-TEK enzyme software). 70
Table 16. Estimated relative amounts of secondary structural components of recombinant wild type *M. avium* DHFR and and D31 and L32 mutants. The fractions of the different structural components were calculated from the data shown in Figure 7 using the program Selcon3. 70

LIST OF FIGURES

Figure 1.Tetrahydrofolate biosynthesis and its role in cell metabolism. Enzymes for each step are given with their EC numbers. Examples of common antifolates that inhibit dihydrofolate reductase are given in box above reaction formula. 2
Figure 2. Chemical structures of the natural substrate folate of DHFR as well as the folate like inhibitors trimethoprim and methotrexate 3
Figure 3. Chemical structure of 2,4-diamino-5-methyl-5-deazapteridines that have been shown to be effective against *M. avium* (58, 59). 3
Figure 4. Multiple sequence alignment of *M. avium* DHFR with other prokaryotes (truncated). Sequences from GenBank. Accession numbers in brackets. *S. epidermidis* (Z48233), *S. aureus* (Y07536), *H. influenzae* (X84207), *B. subtilis* (L77246), *B. anthracis* Sterne, (AAT40581) *L. lactis* (X60681), *E. coli* (Z50802), *M. avium* (AF006616), *L. casei* (M10922). (Source: (69). 7
Figure 5. *Mycobacterium avium* DHFR (EC 1.5.1.3) partial sequence of recombinant wild type p807 aligned with mutations at position D31 13
Figure 6. *Mycobacterium avium* DHFR (EC 1.5.1.3) partial sequence of recombinant wild type p807 aligned with mutations at position L32..... 17
Figure 7:Far-UV CD spectra of recombinant wild type and mutant *M. avium* DHFR. Spectra were acquired in 20mM sodium phosphate, 100mM NaCl, pH 7.4 and 25 °C. For clarity the spectra are represented in two panels. With exception of the spectrum for the L32D mutant, which was obtained from a single protein sample, the spectra shown represent the average obtained from at least two independent protein preparations. Protein names and corresponding symbols are indicated in the figure. 49
Figure 8:Semi-automated purification scheme of recombinant wild type DHFR on His-Bind resin (Novagen) with a linear gradient of 5-500 mM imidazol..... 50
Figure 9:Determination of Michaelis-Menten parameters K_m(FAH2) and V_{max}(FAH2) of recombinant wild type *M. avium* DHFR (p807) at pH 7.0 and 30°C using the non-linear curve fit program Enzfitter (Biosoft, UK). Reaction was initiated by addition of enzyme after the substrates dihydrofolate and NADPH were incubated at 30°C for 1 minute. Absorbance was measured at 340 nm for minute in a Spectronic Genesis 5 spectrophotometer in kinetic mode with 10 second reading intervals. 57

Figure 10:Growth curve at 37°C and 225 rpm of DHFR-deficient *E. coli* strain MG1655*folA::kan3* transformed with recombinant wild type *M. avium* DHFR (p807), D31 mutants and the controls (V76A and pET15b vector only). Growth in the presence of thymidine (A) and growth in the absence of thymidine (B)..... 60
Figure 11:Growth curve at 37°C and 225 rpm of DHFR-deficient *E. coli* strain MG1655*folA::kan3* transformed with recombinant wild type *M. avium* DHFR (p807), L32F mutant and control pET15b vector only. Growth in the presence of thymidine (A) and growth in the absence of thymidine (B)..... 67
Figure 12: Four parameter curves for determination of IC50 relative concentrations of SRI compound 8858 for recombinant wild type, L32D and L32A mutants of *M. avium* DHFR..... 69

CHAPTER I

INTRODUCTION

Background

Dihydrofolate reductase (DHFR, EC 1.5.1.3) is an enzyme found in both prokaryotes and eukaryotes and is essential in the folate biosynthetic pathway (64). DHFR catalyzes the NADPH dependent reduction of dihydrofolate (H_2F) to tetrahydrofolate (H_4F) (Figure 1). The reduction of H_2F to H_4F is a universal requirement for the maintenance of an intracellular reduced folate pool (Figure 1)(24, 41). Intracellular reduced folates are important in one-carbon transfer reactions necessary for the biosynthesis of DNA, RNA and protein (Figure 1) (41).

Due to this important role, DHFR has long been an important therapeutic drug target in anticancer (9), antibacterial (9) and antimalarial (52) treatment. Substrate analogues with high binding affinities exhibit effective inhibition that results in the depletion of the pool of reduced folates (41).

Various antifolate inhibitors for DHFR have been used in the past. Methotrexate is a potent inhibitor of most DHFRs and its inhibitory action is based upon its structural similarity to folate (Figure 2). Trimethoprim is an effective inhibitor of bacterial DHFRs, but is not effective against human DHFR; its structure is also similar to dihydrofolate (Figure 2). Another example of effective antifolates is the class of compounds generally referred to as deazapteridines. Examples of some of these inhibitors (e.g., 2,4-diamino-5-

methyl-5-deazapteridines) that have been shown to be effective against *Mycobacterium avium* are shown in Figure 3.

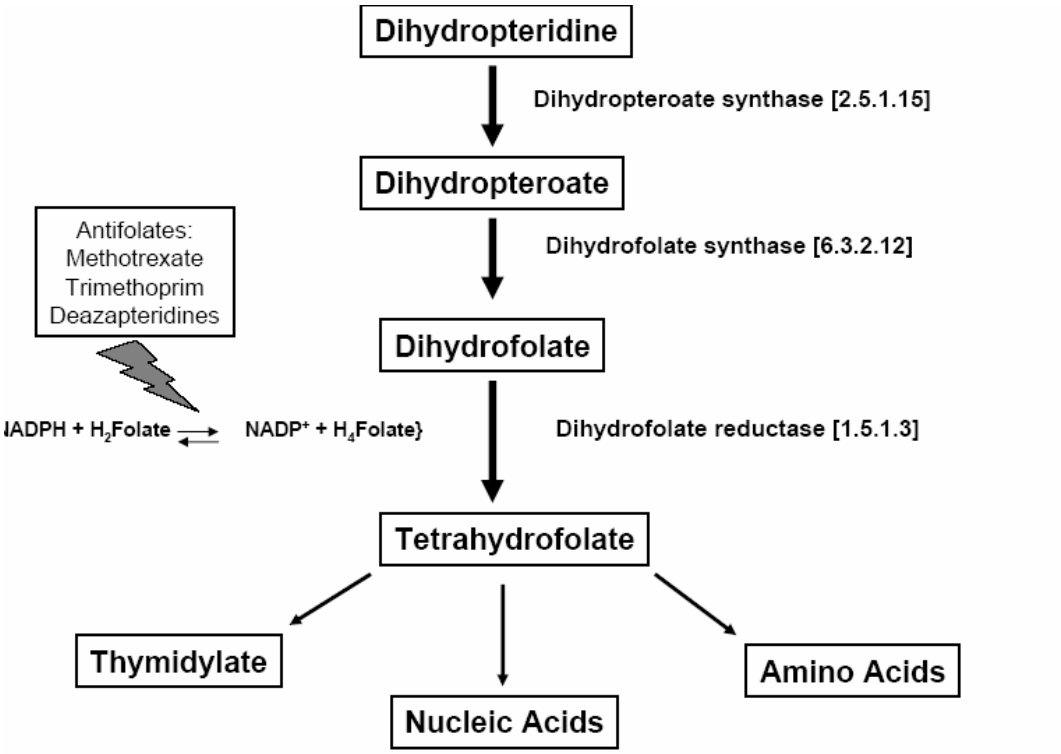

Figure 1**.**Tetrahydrofolate biosynthesis and its role in cell metabolism. Enzymes for each step are given with their EC numbers. Examples of common antifolates that inhibit dihydrofolate reductase are given in box above reaction formula.

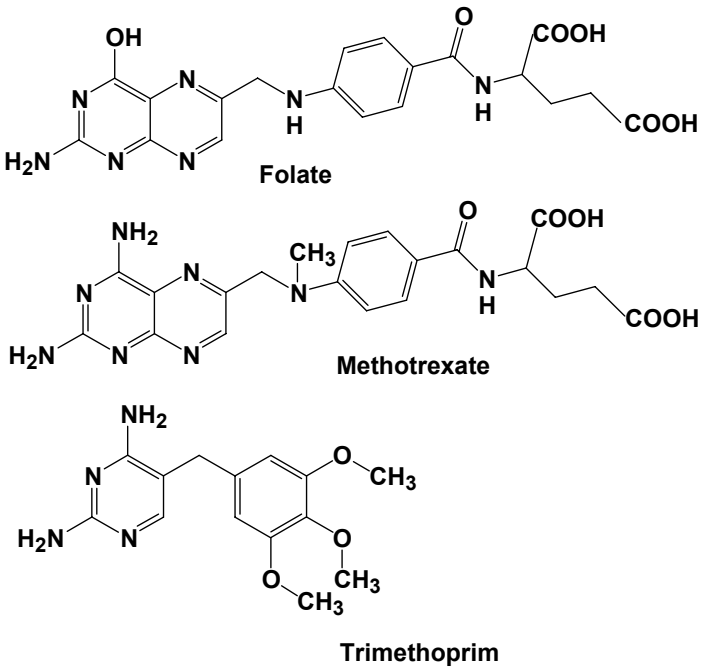

Figure 2**.** Chemical structures of the natural substrate folate of DHFR as well as the folate like inhibitors trimethoprim and methotrexate

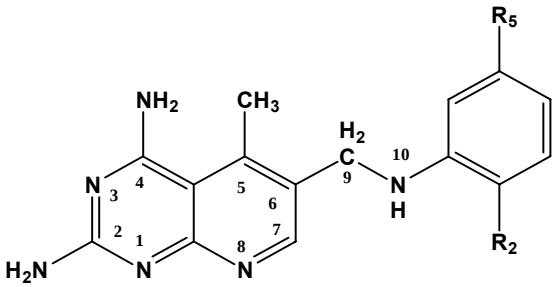

SRI 8858: R_2 and R_5 are $-OCH_2CH_3$

SRI 20730: R_2 and R_5 are $-OCH_2CH_2CH_3$

Figure 3**.** Chemical structure of 2,4-diamino-5-methyl-5-deazapteridines that have been shown to be effective against *M. avium* (58, 59)**.**

Table 1. IC_{50} for trimethoprim for DHFR of various organisms.

Organisms	IC_{50} (nM)	Reference
Escherichia coli	7	(46)
Staphylococcus aureus	5	(46)
Mycobacterium avium	4100	(56, 57)
Chicken	470000	(46)
Mouse	280000	(46)
Human	490000	(46)

As stated above, trimethoprim is an effective antibacterial agent. This drug is effective primarily because of its selective action against various bacterial DHFRs as opposed to eukaryotic DHFRs (Table 1)(27).

Mycobacterium avium has become a serious opportunistic pathogen that causes significant systemic infection in persons infected with HIV (20, 23, 28, 49). Although trimethoprim is an effective therapy for some bacteria, it has poor activity against mycobacteria, including *Mycobacterium avium* (15, 58).

This general resistance of *M. avium* and other mycobacteria to trimethoprim and other antituberculous drugs coupled with the emergence of multidrug resistant clinical isolates of *M. tuberculosis* (20, 55) is evidence for the urgent need for new antimycobacterial

drugs. The development of new antifolates, particularly against mycobacteria, has therefore revived interest in DHFR as a drug target (15, 32, 35, 36, 42, 58, 59). *Mycobacterium avium* DHFR gene (*folA*) has previously been cloned and sequenced and submitted to GenBank under accession number AF006616 (69). It has an open reading frame of 543 bp and a MW of 20kDa. *Mycobacterium avium* DHFR amino acid sequence differs from *M. tuberculosis* and other bacteria in the sense that it has a C-terminal tail of 13 residues with no counterparts in *M. tuberculosis* or other bacteria (33). There is currently no published X-ray crystal structure of the *M. avium* DHFR, however, Kharkar *et al.* (33) have published an homology model of *M. avium* DHFR that was constructed /computed on the basis of *M. tuberculosis* DHFR, using modified Needleman and Wunsch methodology and assessment of stereochemistry by a Ramachandran plot as well as with existing experimental data.

The overall primary sequence identity among DHFR of different organisms may vary greatly as indicated in Table 2 and may even be as low as 17 – 20% (35). The overall primary structure identity of DHFR in eukaryotes and prokaryotes are usually around or less than 25% (61). Primary structure identities among vertebrates are usually high (65). The primary sequence identity of human with mouse, chicken and bovine DHFR is 89, 74 and 81%, respectively. (37). Compared to *M. tuberculosis* and *E. coli* the primary sequence identity of human DHFR is only 26 and 28%, respectively. Even among bacteria DHFR sequence identities can be very low. *Escherichia coli* and *Lactobacillus casei* DHFR have only about 28% primary sequence identity (34). On the other hand *M. avium* and *M. tuberculosis* have around 70% primary sequence identity. Despite such

large variation in primary sequence homologies, the tertiary structure of *E. coli* and *L. casei* DHFR is remarkably similar (34) .

Table 2**.** Comparison of overall amino acid sequence identity in DHFR of various species.

DHFR species compared		**% overall identity**	**Reference**
M. avium	*M. tuberculosis*	~70	(33)
M. avium	*M. leprae*	62	(69)
M. tuberculosis	Human	26	(35)
E. coli	*L. casei*	29	(8)
Human	*E. coli*	28	(53)
Human	Mouse	89	(37)

All known DHFRs have the same structural features, consisting of a dominant central ß-sheet with 4 flanking α-helices (35, 39). Major structural differences occur mostly on the exterior (35). *Mycobacterium avium* DHFR as revealed in the model of Kharkar *et al.* (33) show the same structural features, common to all other DHFRs.

Although, as indicated in Table 2, the overall sequence identity between *M. tuberculosis* and human DHFR is only 26%, the sequence identity in the binding cavity is 55% (35).

Escherichia coli and *L. casei* also only have 28% primary sequence identity; however, this increases to 50% in the binding cavity (65).

Multiple sequence alignments of all known DHFRs show very strong conserved amino acid residues for both vertebrates and bacteria. Figure 4 below shows a part of the amino acid sequence alignment of *M. avium* DHFR with several other bacterial species with a conserved aspartic acid in position 31 of *M. avium*. Aspartic acid 31 (D31) of *M. avium* is conserved in this position for all known bacterial DHFRs; it is replaced by glutamic acid in the same structural position in vertebrate DHFRs (64). The structurally equivalent position of *M. avium* D31 is D27 in *E. coli*, D26 in *L. casei* and E30 in human DHFR. DHFR in vertebrates has a conserved aromatic residue (tyrosine or phenylalanine) at position 31 (F31 in humans), while a leucine residue is found in the same structural position in bacteria (L28 in *E. coli*, L27 in *L. casei* and L32 in *M. avium*) (47, 69).

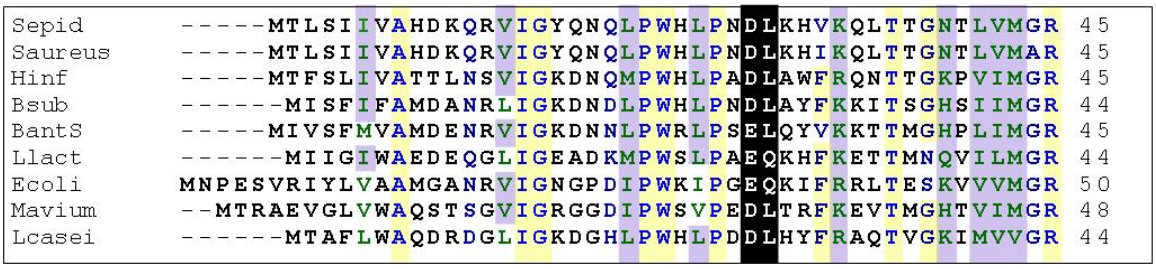

Figure 4**.** Multiple sequence alignment of *M. avium* DHFR with other prokaryotes (truncated). Sequences from GenBank. Accession numbers in brackets. *S. epidermidis* (Z48233), *S. aureus* (Y07536), *H. influenzae* (X84207), *B. subtilis* (L77246), *B. anthracis Sterne,* (AAT40581) *L. lactis* (X60681), *E. coli* (Z50802), *M. avium* (AF006616), *L. casei* (M10922). (Source: (69)**.**

Both of these conserved residues are in the DHFR binding cavity. The DHFR binding cavity is located in a very hydrophobic pocket. The highly conserved carboxylic acid

(D31 in *M. avium*, D27 in *E. coli*, D26 in *L. casei* and E30 in humans) is the only ionizable residue in the active site of all known DHFRs (13, 38, 45, 46). The conserved phenylalanine (F31 in human DHFR) or leucine (L32 in *M. avium*) residues together with other hydrophobic residues in the binding cavity are thought to ensure and maintain an efficient hydrophobic environment which is necessary for hydrophobic interactions with both the substrate and inhibitors (46).

Changes in the conserved carboxylic acid have been shown to significantly decrease catalytic activity (1, 3, 11, 22, 30, 34, 40, 44, 46, 60, 64). Replacement of the aromatic residues have also been shown to weaken the hydrophobic interactions (14, 21, 29, 46, 47, 63).

The conserved aspartic acid (D27 in *E. coli*) was observed by Matthews *et al.* (39) and they were first to suggest that this aspartic acid must play a role in catalysis. Matthews *et al.* (38) published an X-ray crystal structure of *L. casei* DHFR and proposed that D27 of *E. coli* serves as proton donor in the enzyme reaction. Since then mutational studies of this conserved carboxylic acid residue have been done for several species and the importance of this residue confirmed (1, 3, 11, 22, 30, 34, 40, 44, 46, 60, 64).

Mathews *et al*. (38, 39) published X-ray crystal structures of *E. coli and L. casei* complexed with methotrexate (MTX). They showed that in both cases the *p*-aminobenzoyl portion of the drug was in a hydrophobic pocket of the active site and also identified a number of residues that are involved in the binding of this drug. Leucine 27 (*L. casei*) and leucine 28 (*E. coli*) were among the side chains making contact with the pteridine ring of methotrexate.

Baccanari *et al*. (4) reported on 2 DHFR isozymes isolated from a trimethoprim resistant *E. coli* and showed that the only difference between them was a single amino acid substitution. Form 1 had a leucine residue in position 28 (L28), while Form 2 had an arginine (R28). Both forms were very different in their binding and kinetic properties. Trimethoprim was shown to be a better inhibitor of Form 1.

Dale *et al.* (16) also reported a single active site amino acid substitution in *Staphylococcus aureus* DHFR that resulted in resistance to trimethoprim. A common mutation in trimethoprim resistant clinical isolates of *S. aureus* from diverse geographical regions was a substitution of phenylalanine 98 to tyrosine (F98Y). Several studies (17, 51) have identified 2 plasmids in staphylococci that carried trimethoprim-resistant DHFR genes with a single difference, namely a tyrosine in position 98. Dale *et al.* (16) then isolated chromosomal DNA of *S. aureus* DHFR and introduced the same F98Y mutation through site-directed mutagenesis. They found these mutants to be resistant to trimethoprim. In conclusion they could show in the X-ray crystal structure that the tyrosine in position 98 interferes with the hydrogen bonding of leucine 5 and phenylalanine 92; these residues are in close contact with and bind to the inhibitor.

Numerous studies then investigated hydrophobic interactions within the binding site of DHFR and through site-directed mutagenesis and X-ray crystallography identified functional roles of specific residues (14, 44, 47, 48, 63). The overall conclusion from these studies was that there were 4 key residues that ensured efficient hydrophobic interaction with inhibitors. One of those residues was L28 in *E. coli* and L27 in *L. casei* (46).

The tyrosine 98-dependent mechanism of resistance against trimethoprim that was described earlier (16) shows that detailed knowledge at molecular and structural level of resistance mechanisms could be useful in rational design of inhibitors that could be effective against resistant DHFRs.

Wyss *et al.* (67) reported novel 2,4-diaminopyrimidines with high activity against trimethoprim-sensitive and trimethoprim-resistant *Streptococcus pneumoniae* DHFR. They also showed that introduction of methoxy substitutents on the drug led to enhancement of inhibitory activity compared to non-substituted compounds. They further found that selection of compounds from structure-based libraries led to significantly more hits and those hits were significantly more potent than libraries based on diversity.

Mycobacterium avium is inherently resistant to trimethoprim other antibiotics and a variety of antimycobacterial agents (43, 49). However, trimethoprim is differently selective for bacterial DHFR over mammalian DHFR (27). Although overall tertiary structure for all known DHFRs are very similar, sufficient differences exist between species within the binding site that could be exploited to design inhibitors that are more selective (14).

Suling *et al*. (58, 59) reported on antimycobacterial activity of 2,4-diamino-5-methyl-5-deazapteridine derivatives (DMDPs). In the first study, 4 of the 12 compounds showed selective activity against *Mycobacterium tuberculosis* and *Mycobacterium avium*, compared to vero cell toxicity. In the second study 77 compounds with key modifications investigated the binding and selectivity for *M. avium* DHFR compared to human DHFR. Although these compounds showed good activity against *M. avium* DHFR, they

concluded that compared to results reported for trimethoprim it would be necessary to further improve the selectivity ratio at least 10-fold so that the drugs could compare to the selectivity ratios of trimethoprim of other bacteria.

Although there is currently no published crystal structure of *M. avium* DHFR, the model of *M. avium* DHFR that was constructed /computed on the basis of *M. tuberculosis* DHFR by Kharkar *et al.* (33) also identified structurally and functionally important residues, particularly those important for binding of the previously reported deazapteridine inhibitors (58, 59). Site-directed mutagenesis studies of those residues could further verify the importance of specific amino acid residues in the binding and catalysis.

Leucine 32 in *M. avium* DHFR was identified as one of the residues that interact with the aminopteridine ring, the *p*-aminobenzoyl ring and the glutamate moiety of methotrexate (33.). This is consistent with current knowledge as reviewed above, since leucine 32 of *M. avium* is the structurally equivalent position of L28 in *E. coli* and L27 in *L. casei* (46).

Objectives

Based therefore on the above review of literature and crystallographic data of known DHFRs, as well as the proposed homology model of *M. avium* DHFR by Kharkar *et al.* (33.), this study hypothesizes (1) a functional role for aspartic acid 31 (D31) in the binding of the natural substrate and (2) a functional role for leucine 32 (L32) in the binding of antifolates such as trimethoprim as well as the 2,4-diamino-5-deazapteridines deazapteridines described previously for *Mycobacterium avium* DHFR .

Hypothesis 1

In order to test hypothesis 1, D31 of the recombinant wild type *M. avium* DHFR was substituted by alanine (D31A), glutamic acid (D31E), glutamine (D31Q),

asparagine (D31N) and leucine (D31L) using site-directed mutagenesis (Figure 5). The recombinant and mutant enzymes were then expressed in *E. coli* and purified and the functionality of the mutants determined in comparison to the recombinant wild type in the procedures described in the materials and methods section of this study. Table 3 summarizes the expected effects of the D31 mutations on the mutant enzyme's functionality.

Previous experiments have shown that aspartic acid 27 in *E. coli* (conserved carboxylic acid among known bacterial DHFRs) participates in proton transfer between solution and substrate (30, 57, 66). Changing aspartic acid 31 (D31) in *M. avium* DHFR to glutamic acid (D31E) will retain the nature of this charge, however, the side chain has an additional methylene group, extending the side chain by approximately 1 Å. If there is flexibility in terms of geometry within the binding cavity, then this mutation should not have an effect on the enzyme-substrate binding and therefore should not affect the enzyme activity.

Substituting aspartic acid 31 with glutamine (D31Q) will result in a similar geometry as glutamic acid (D31E), but without the carboxylic acid group. With the importance of the carboxylic acid group in proton transfers, this mutation (D31Q) should render the DHFR inactive.

Mutating D31 to alanine (D31A) will eliminate the carboxylic acid group completely and remove the potential proton source. This should affect the enzyme activity negatively.

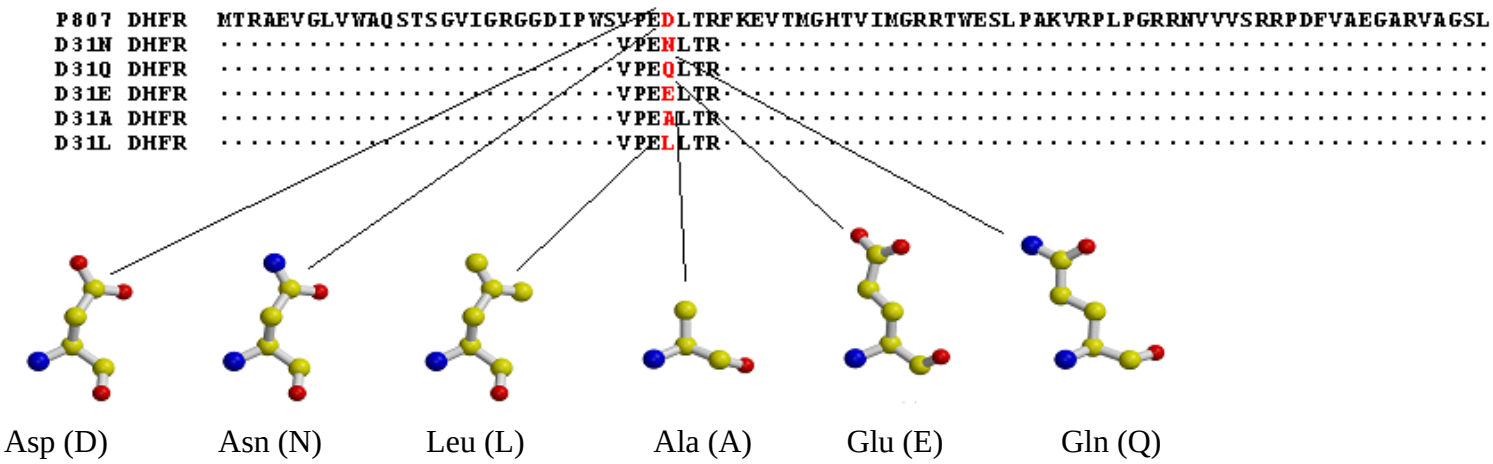

Figure 5 *Mycobacterium avium* DHFR (EC 1.5.1.3) partial sequence of recombinant wild type p807 aligned with mutations at position D31

Substituting aspartic acid 31 with asparagine (D31N) will retain the size and geometry, but will remove the negative charge of the carboxylic acid group. The residue will, however, be polar. Since aspartic and glutamic acid are the only 2 amino acids with negative carboxylic side groups and aspartic acid is highly conserved in this position, it is expected that this mutation will also render the resulting enzyme inactive.

Changing D31 to leucine (D31L) will also retain the same size and geometry, but will result in a non polar side chain. This recombinant mutant *M. avium* DHFR is also expected to be dysfunctional.

It is necessary to perform a negative control, i.e. construct a recombinant mutant *M. avium* DHFR with the same technique, with a mutation that should not have any effect on the enzyme's activity. This will verify that the loss in enzyme activity is a result of the affected mutations and not of some side effect of the procedure. For this**,** Valine 76 will be modified to alanine (V76A). Valine 76 is sufficiently far away from the enzyme's binding site and is exposed on a surface loop with no interaction with other secondary structural elements.

Table 3.Mutations of D31 and their expected effects on functionality of *M. avium* DHFR

Mutation	Change in side group	Hypothesis
D31E	Larger, but same charge	If flexibility allowed in active site, no effect expected in activity
D31Q	Larger, no charge, but polar	COOH group important, therefore enzyme dysfunctional
D31A	Smaller, no charge	COOH eliminated, enzyme dysfunctional
D31N	Same size and geometry, remove negative charge, remain polar	dysfunctional enzyme
D31L	Same size and geometry, no charge, nonpolar	dysfunctional enzyme
V76A	"negative control"	No effect on activity

Hypothesis 2

Hypothesis 2 was tested similarly by modifying L32 of the recombinant wild type *M. avium* DHFR by site-directed mutagenesis to phenylalanine (L32F), alanine (L32A) and aspartic acid (L32D) (Figure 6) and assessing both the functionality of the enzyme as well as its interaction with trimethoprim and selected deazapteridine inhibitors in the procedures described in the following chapter of this study. The expected effects of the L32 mutations of the functionality of the mutant enzyme are summarized in Table 4.

The equivalent position of *M. avium* leucine 32 in human DHFR is phenylalanine 31 (F31). Changing leucine 32 in *M. avium* DHFR to phenylalanine (L32F) would

not change the hydrophobic nature, but increase the size of the side chain. If F31 in humans contributes to trimethoprim resistance, this mutation should decrease selectivity of the mutant for trimethoprim.

Given the proposed role of leucine 32 in interacting with inhibitors, the L31A mutations would remove this important hydrophobic side chain and lessen the affinity of the inhibitor, thereby also decreasing selectivity.

The L32D mutation will not only remove the hydrophobic side chain of the wild type, but also introduce a charged group into an overall hydrophobic region. It is expected that the loss of hydrophobicity will negatively affect inhibitor binding and decrease selectivity.

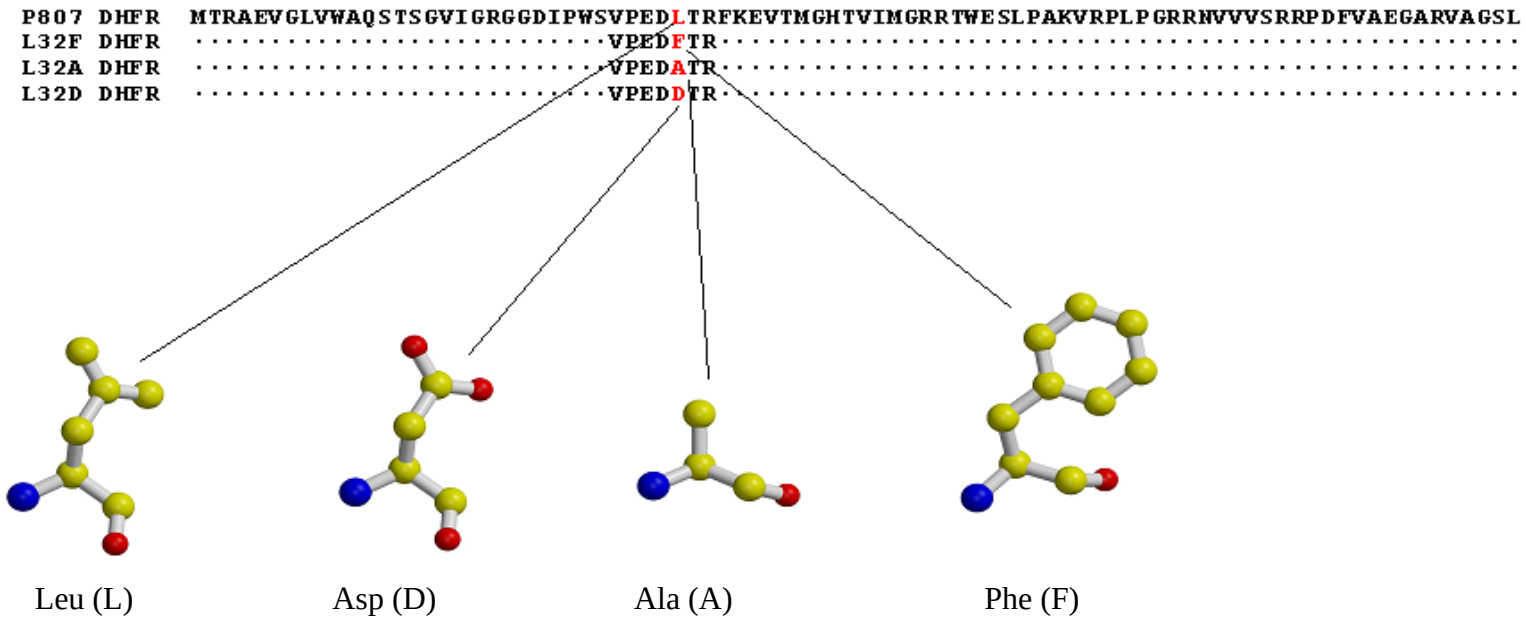

Figure 6 *Mycobacterium avium* DHFR (EC 1.5.1.3) partial sequence of recombinant wild type p807 aligned with mutations at position L32

Table 4**:** Mutations of L32 and their expected effects on functionality of *M. avium* DHFR

Mutation	**Change in side group**	**Hypothesis**
L32F	Larger, but still hydrophobic	No effect on enzyme activity expected Effect on inhibitor IC_{50} expected
L32A	Smaller, no charge, remove hydrophobic residue	No effect on enzyme activity or inhibitor selectivity expected
L32D	Same size, remove hydrophobicity, introduce charge	No effect on enzyme activity expected Effect on inhibitor IC_{50} expected

CHAPTER 2

MATERIALS AND METHODS

Bacterial strains used

E. coli JM109 (Promega)

E. coli BL21(DE3)pLysS (Promega)

*E. col*i BMH71-18*mut*S (Promega)

E. coli MG1655

E. coli MG1655*folA::kan3*

Mycobacterium avium DHFR gene (*folA*)

Mycobacterium avium folA gene has first been identified, cloned and sequenced and submitted to GenBank under accession number AF006616 (69). It has an open reading frame of 543 bp and a MW of 20kDa. Functionality of the recombinant enzyme was shown in vitro in a standard enzyme assay as well as in vivo through functional complementation (69) .

Plasmid vector construct p807 for recombinant *M. avium* DHFR

Plasmid DNA of the previously cloned *M. avium folA* gene was available in the Lab of Dr. W. Barrow. The *M. avium folA* gene had previously been cloned into the pET15b vector (Novagen) at the Nde1 and BamH1 restriction sites. (69). The pET15b vector contained an N-terminal His-tagged leader sequence.

This plasmid construct consisting of the pET15b vector with the *M. avium folA* gene insert, will serve as the recombinant wild type *M. avium* DHFR.

Validation (Verification) of recombinant wild type *M. avium* DHFR

E. coli JM109 competent cells (Promega) were transformed with recombinant wild type DHFR plasmid construct p807 DNA according to Promega *E. coli* competent cells Standard Transformation Protocol.

Transformation

Sterile polypropylene Falcon® 2059 tubes were chilled on ice. High efficiency competent cells (>10^8 cfu/µg) were thawed on ice for five minutes and 100 µl cells transferred to each tube. About 10 ng of plasmid DNA was added to each tube and the tube flicked gently. These tubes were kept on ice for 10 minutes, then heat-shocked for 45-50 seconds in a water bath at exactly 42°C. The reaction was returned to ice for two minutes and 900 µl SOC medium (Novagen) was added to each tube. Tubes were incubated for 60 minutes at 37°C in a shaking incubator at 225 rpm. For each reaction 100 µl was plated undiluted, diluted 1:10 and 1: 100 onto Luria-Bertani (LB) Agar containing 100µg/ml carbenicillin. Plates were incubated at 37°C for 12 – 14 hours.

Overnight cell growth

A single colony was grown overnight in 10 ml LB-Broth with 100 µg/ml carbenicillin in a shaking incubator at 37°C and 225 rpm. Cells were harvested by centrifugation at maximum speed (2135 x g) at 4°C for 10 minutes (Sorval RTH-250 rotor).

Plasmid DNA extraction

Plasmid DNA was extracted using the Wizard® Plus SV miniprep DNA purification system (Promega). The pellet from the overnight culture was resuspended into 250µL cell resuspension solution and vortexed to ensure complete resuspension. Thereafter 250 µl cell lysis solution was added and tubes were mixed by inverting several times until cell suspension cleared. After five minutes 10 µl alkaline protease solution was added and were again mixed by inverting several times. Tubes were incubated at room temperature for 5 minutes and 350 µl Wizard® Plus SV neutralization solution was added and tubes were mixed by inverting. The lysate was centrifuged in a table top microcentrifuge at 14,000 x g for 10 minutes at room temperature. The plasmid DNA was then purified by microcentrifugation using Wizard® Plus SV miniprep spin columns. For each sample a spin column was inserted into a 2 ml collection tube. The supernatant of the prepared lysate was then transferred to the spin column either by decanting or pipetting. Care was taken not to transfer any of the precipitate. The columns were centrifuged at maximum speed (14,000 x g) at room temperature for one minute. The flow through was discarded and the spin columns were reinserted into the collection tubes. Columns were washed by adding 750 µl column wash solution onto each spin column. Columns were again centrifuged at maximum speed (14,000 x g) at room temperature for one minute. The flow through was discarded and the process repeated with 250 µl column wash solution, but this time centrifuged for 2 minutes. The spin columns were transferred to sterile 1.5 ml centrifuge tubes. To elute the plasmid DNA 100 µl nuclease-free water was added to the spin columns and columns were centrifuged

at 14000xg for 1 minute at room temperature. After determining the plasmid DNA concentration and purity, the plasmid DNA was stored at -20°C until further use.

Determining plasmid DNA concentration and purity

Plasmid DNA concentration was determined in a GeneQuant proRNA/DNA calculator (Amersham) using quartz microcapillaries.

Restriction endonuclease digestion and agarose gel electrophoresis

Extracted plasmid DNA was subjected to restriction endonuclease double digestion with BamH1 and Nde1 and agarose gel electrophoresis in order to verify the presence of the insert. The reaction setup is described in Table 5. The same plasmid DNA was also sequenced in order to confirm the insert as the DHFR gene.

Table 5**.** Restriction endonuclease reaction setup for excising the *folA* gene from the p807 plasmid construction

	pET15b undigested	pET15b digested	p807 undigested	p807 digested
Sterile dH_2O	15.8 µl	15.6 µl	7.3 µl	10.5 µl
BamH1 Buffer	2 µl	2 µl	2 µl	2 µl
100X BSA (100mg/ml)	0.2 µl	0.2 µl	0.2 µl	0.2 µl
Template DNA	2 µl (~ 1µg)	2 µl (~ 1µg)	10 µl (1µg)	10 µl (1µg)
BamH1	-	0.25 µl (5 U)	-	0.25 µl (5 U)
Nde1	-	0.25 µl (5 U)	-	0.25 µl (5 U)

The 20 ml reaction tubes were incubated in a 37°C water bath for 2 hours. After digestion 4 ml 6X loading buffer (Promega). A 1.2% agarose gel was prepared by adding 30 ml 1 X TAE buffer to 0.36g agarose and heating it in a microwave until boiling (about 1 minute). After cooling to about 50°C 1.5 µl ethidium bromide (Promega: 10mg/ml) was added to the agarose and the gel was poured in a flat bed tray 7x6.2x1 cm. Electrophoresis was carried out for 50 minutes at 75V in a mini-sub® cell GT electrophoresis chamber (Promega) using 1X TAE buffer.

Sequencing

Mutations were confirmed by sequencing the full length of the *folA* gene insert of the pET15b vector using T7 forward and reverse primers. Sequencing was done at either the Recombinant DNA/Protein Resource Facility of Oklahoma State University (Stillwater, OK) or at the Oklahoma Medical Research Foundation (OMRF, Oklahoma City, OK).

Pilot expression of recombinant wild type *M. avium* DHFR

Transformation

BL21(DE3) pLysS competent cells (Promega) were transformed with recombinant DHFR plasmid construct p807 DNA, according to Promega *E. coli* competent cells Standard Transformation Protocol as described above (Section 2.4.1). Each transformation reaction was plated undiluted onto LB-Agar containing 100 µg/ml carbenicillin and 34 µg/ml chloramphenicol and incubated overnight at 37°C.

Growth and IPTG induction

A single colony was grown overnight in 10 ml LB-Broth with 100 µg/ml carbenicillin and 34 µg/ml chloramphenicol in a shaking incubator at 37°C and

225 rpm. From each 10 ml overnight culture 500 µl was used to inoculate 10 ml LB-Broth containing 100 µg/ml carbenicillin and 34 µg/ml chloramphenicol. The culture was grown in a shaking incubator at 37°C and 225 rpm until an OD600 of 0.6 - 0.7 was obtained. At this point the growing culture was divided into 2 x 5ml using sterile 50 ml conical tubes. From each culture 500 µl were removed as a pre-induced sample and non-induced sample at zero time. Samples were centrifuged at 16,000 x g for 20 minutes at 4°C; the supernatants were discarded and the pellets stored at -20°C until used. Only one of these cultures was induced by adding 1 mM IPTG (final conc.). Both cultures (induced and non-induced) were continued to grow at 28°C in a shaking incubator at 225 rpm for 21-24 hours. At this point another 500 µl was removed as induced and non-induced sample at time 21 or 24 hours and centrifuged as above. After 24 hours cells were harvested by centrifugation at 4°C at maximum speed (2135 x g) for 20 minutes (Sorval RTH-250 rotor).

BugBuster protein extraction

BugBuster Protein Extraction Reagent Kit and Benzonase nuclease (Novagen) and Protease Inhibitor cocktail III (Calbiochem) were used to lyse the cells and extract the soluble protein from the pellets. Pellets were resuspended in 100 µl Bugbuster® Protein Extraction Reagent and 0.1 µl Benzonase Nuclease reagent and incubated on a shaker at room temperature for 15 minutes. The cell lysate was centrifuged at 4° at 16,000 x g for 20 minutes. The supernatant was collected and stored at -20°C until use in SDS-PAGE.

Polyacrylamide gel electrophoresis (SDS-PAGE)

Samples for SDS-PAGE were prepared by adding 10 µl 2x SDS-sample buffer (Novagen) to 10 µl extract. Samples were heated at 95°C for 5 minutes in a heating block and thereafter kept on ice for at least 10 minutes before electrophoresis. Electrophoresis took place under denaturing conditions on a 12.5% (w/v) polyacrylamide gel.

Composition of gels and solutions were as follow:

Separating gels

Acrylamide/N'N-methylene bisacrylamide	12.5% (w/v)
Tris-HCl, pH 8.8	375 mM
SDS	0.1% (w/v)

Stacking gels

Acrylamide/N'N-methylene bisacrylamide	6.0% (w/v)
Tris-HCl, pH 6.8	125 mM
SDS	0.1% (w/v)

Gels were polymerized by the addition of N,N,N',N',-Tetramethylene ethylene diamine (TEMED) and Ammonium persulphate (APS) 10%w/v as indicated below:

	Separating gel	Stacking gel
N,N,N',N',-Tetramethylene ethylene diamine (TEMED)	0.1% (v/v)	0.1% (v/v)
Ammonium Persulphate (APS) 10%w/v	0.1% (v/v)	0.1% (v/v)

SDS sample buffer

125mM Tris-HCl, pH 6.8,

2.0% (w/v) SDS

20% (w/v) glycerol

0.001% (w/v) Bromophenol blue

0.05% (w/v) ß-mercaptoethanol

Electrophoresis running buffer

25 mM Tris-Hcl, pH 8.3

192 mM Glycine

0.1% (w/v) SDS

Gels were run for 45 minutes at 200 Volts constant and then stained for several hours or over night in Coomassie blue R-250 solution [0.1% (w/v) Coomassie blue R-250, 50% (v/v) methanol, 10% (v/v) acetic acid].

The gels were destained for several hours until the gels had a clear and transparent background (Destain solution: 40% (v/v) methanol and 10% (v/v) acetic acid).

Site-directed mutagenesis

The p807 plasmid construct of the *M. avium* folA gene was used as template DNA for oligonucleotide-based site-directed mutagenesis of aspartic acid 31 (D31) and leucine 32 (L32) as well as the control mutation valine 76 (V76), using the GeneEditor Protocol Kit (Promega).

Design and synthesis of mutagenic oligonucleotides

Mutagenic oligonucleotides were designed in accordance with Promega's GeneEditor Kit recommendations (Promega TM 047). Single base changes should have about 17 – 20 bases with about 8 – 10 matched bases on either side. For 2 or more mismatches, oligonucleotides of 25 or longer bases are required with about 12 – 15 matched bases on either side. The mismatch should be as close to the center as possible. The following mutagenic oligonucleotides were commercially synthesized and PAGE purified (IDT) (Table 6).

Table 6**.** *M. avium fol*A D31 and L32 mutants and primers used to construct them.

Mutation	Primers, 5'-3', with mutational codon highlighted in **bold**
D31E	CGAG**GAG**CTCACCCGGTTCAAG
D31Q	CGTGCCCGAG**CAA**CTCACCCGGTTC
D31A	CGAG**GCC**CTCACCCGGTTCAAAG
D31N	GCCCGAG**AAC**CTCACCCGGTTCAAAG
D31L	CGTGCCCGAG**CTC**CTCACCCGGTTCAAAG
V76A	CCCGACTTC**GCC**GCCGAGGGG
L32F	GCCCGAGGAC**TTC**ACCCGGTTC
L32A	GCCCGAGGAC**GCC**ACCCGGTTC
L32D	GCCCGAGGAC**GAC**ACCCGGTTC

5'-Phosphorylation of mutagenic oligonucleotides

All mutagenic oligonucleotides were 5'-phosphorylated prior to the mutagenesis procedure. The reaction set up and procedure were as follow:

Mutagenic oligonucleotide	100pmol	0.5µl
Kinase 10X Buffer		2.5µl
T4 Polynucleotide Kinase	5U	0.5µl
ATP, 10mM		2.5µl
Sterile deionized H_2O to final volume of		25µl

The reaction was incubated in a water bath at 37°C for 30 minutes and then heated to 70°C in a heating block for 10 minutes in order to inactivate the T4 Polynucleotide kinase. The reaction product was stored at -20°C until used.

Mutagenesis reaction

Alkaline denaturation (dsDNA)

The recombinant wild type plasmid DNA (p807) was used as a template to generate all the mutants. GeneEditor control DNA (pGEM11z(f) vector) was also denatured during the same procedure. Non-denatured controls did not contain the 2M NaOH, 2mM EDTA, but were otherwise treated in the same manner. The remaining volume was made up with sterile deionized H_2O. The following reaction setup generated enough denatured DNA for 10 mutagenesis reactions:

dsDNA template	0.5pmol (approx. 2µg)
2M NaOH, 2mM EDTA	2µl
sterile deionized H_2O to final Volume	20µl

The reaction was incubated at room temperature for 5 minutes, and then 2µl of 2M ammonium acetate (pH4.6) and 75µl of 100% cold (4°C) ethanol were added. The reaction was further incubated at -70°C for 30 minutes. The reaction was centrifuged at 16,000 x g in a micro centrifuge for 15 minutes at 4°C. The pellets were drained and washed with 200µl of 70% ethanol (4°C) and centrifuged as above. The pellets were dried under vacuum in a speedvac for 30 minutes with 10 minutes heating time at medium level. Pellets were suspended in 100 µl TE buffer (pH 8.0) and a 10 µl sample was analysed for denaturation on an agarose gel before the next step in the procedure.

Agarose gel electrophoresis

A 0.8% agarose gel was prepared by adding 30 ml 1 X TAE buffer to 0.24g agarose and heating it in a microwave until boiling (about 1 minute). After cooling to about 50°C, 1.5 µl ethidium bromide (Promega: 10mg/ml) was added to the agarose and the gel was poured in a flat bed tray 7x6.2x1 cm. Electrophoresis was carried out for 50 minutes at 75V in a mini-sub® cell GT electrophoresis chamber (Promega) using 1X TAE buffer

Oligonucleotide hybridization

The GeneEditor™ mutagenesis system is supplied with two selection oligonucleotides: Top- and Bottom Strand. The Top Strand is identical in sequence to the mRNA that encodes for the ampicillin resistance (ß-lactamase gene) which is carried as a selection marker on the plasmid vector. Both the mutagenic and the selection oligonucleotide have to hybridize to the same strand. The orientation of the inserted gene and the ampicillin resistance gene of the vector determine which of the two selection oligonucleotides to use. The *folA*

insert in the pET15b vector and the ampicillin resistance gene in that plasmid vector both had the same orientation, so the selection oligonucleotide Top Strand was used.

For each mutation a separate reaction was set up in an eppendorf tube as indicated below:

Alkaline denatured Template DNA	0.05pmol	10µl
Selection oligonucleotide Top Strand		
(phosphorylated, 2.9ng/µl)	0.25pmol	1µl
mutagenic oligonucleotide		
(Phosphorylated)	1.25pmol	0.31µl
Annealing 10X Buffer		2.0µl
Sterile deionized H_2O to final volumes of		20µl

The mutagenesis control reaction utilizes an oligonucleotide that disrupts the lacZ α-peptide of the control vector (pGEM®-11Zf(+)). *E. coli* JM109 that is transformed with transformants carrying the control mutation will form white colonies on agar media containing X-Gal and IPTG. The reaction set up for the mutagenesis control reaction was as follows:

Alkaline denatured pGEM®-11Zf(+) vector DNA	0.05pmol	10µl
Selection oligonucleotide, Bottom Strand		
(phosphorylated, 2.9ng/µl)	0.25pmol	1µl
lacZ Control Knockout oligonucleotide		
Bottom strand (13.2ng/µl)	1.25pmol	1µl
Annealing 10X Buffer	2.0µl	
Sterile deionized H_2O to final volumes of	20µl	

The hybridization reactions were heated to 75°C for 5 minutes in a water bath and then allowed to cool down to 37°C at a rate of about 1.5°C per minutes. This was achieved by removing about 200 ml of water from the water bath with a beaker, and keeping the reaction tubes in the beaker at room temperature for about 30 – 40 minutes.

Mutant strand synthesis and ligation

Once the annealing reaction had cooled down to 37°C, tubes were centrifuged briefly to collect the contents at the bottom of the tube. In order to complete the strand synthesis (heteroduplex formation), the following components were added to the reaction tubes in the order listed:

Sterile deionized H_2O		5µl
Synthesis 10X Buffer		3µl
T4 DNA Polymerase	5U	1µl
T4 DNA Ligase	1-3U	1µl
Final volume		30µl

These reactions were incubated at 37°C for 90 minutes in a water bath and then kept on ice.

Transformation of BMH 71-18 *mut*S (repair-minus strain)

Transformation and over night growth

Sterile polypropylene Falcon® 2059 tubes were chilled on ice. BMH 71-18 *mut*S competent cells (>10^7 cfu/µg) were thawed on ice or five minutes and 100 µl cells transferred to each tube. About 10 ng of template DNA (1.5µl of each mutagenesis reaction) was added to each tube respectively and the tube flicked gently. These tubes were kept on ice for 10 minutes, then heat-shocked for 45-50 seconds in a water bath at exactly 42°C. The reaction was returned to ice for two minutes and 900 µl room temperature LB broth without antibiotic was added to each tube. Tubes were incubated for 60 minutes at 37°C in a shaking incubator at 225 rpm. For each reaction an overnight culture was prepared by adding 4ml LB medium containing 100 µl of the GeneEditor™ Antibiotic Selection Mix to each transformation reaction. Reactions were incubated for 16 – 18 hours in a shaking incubator (225rpm) at 37°C.

Plasmid DNA extraction

Plasmid DNA was extracted from the BMH 71-18 *mut*S overnight cultures as described above.

Determination of plasmid DNA concentration and purity

Plasmid DNA concentration was determined in a GeneQuant proRNA/DNA calculator (Amersham) using quartz microcapillaries.

Transformation of JM109

Transformation

Sterile polypropylene Falcon® 2059 tubes were chilled on ice. High efficiency competent cells (>10^8 cfu/µg) were thawed on ice or five minutes and 100 µl cells transferred to each tube. For each mutation about 10 ng of plasmid DNA extracted from the BMH 71-18 *mut*S cells was added to each Falcon® 2059 tube and the tube flicked gently. These tubes were kept on ice for 30 minutes, then heat-shocked for 45-50 seconds in a water bath at exactly 42°C. The reaction was returned to ice for two minutes and 900 µl (room temperature) SOC medium (Novagen) was added to each tube. Tubes were incubated for 60 minutes at 37°C in a shaking incubator at 225 rpm. For each reaction, 100 µl was plated undiluted, diluted 1:10 and 1: 100 onto LB Agar containing 125µg/ml carbenicillin and 100µl of the GeneEditor™ Antibiotic Selection Mix for 20 ml LB agar. That mixture was spread onto 20 ml agar and incubated at 37°C for 30 minutes. Plates were incubated at 37°C for 12 – 14 hours.

Overnight cell growth

For each mutation at least 5 isolated colonies were selected and grown separately overnight in 10 ml LB-Broth with 100 µg/ml carbenicillin and 50 µl GeneEditor™ Antibiotic Selection Mix in a shaking incubator at 37°C and 225 rpm (12-14 hours). Cells were harvested by centrifugation at maximum speed (2135 x g) 4°C for 10 minutes (Sorval RTH-250 rotor).

Plasmid DNA extraction

Plasmid DNA was extracted using the Wizard® Plus SV miniprep DNA purification system (Promega) as described above.

Determining plasmid DNA concentration and purity

Plasmid DNA concentration was determined in a GeneQuant proRNA/DNA calculator (Amersham) using quartz micro capillaries

Sequencing

Mutations were confirmed by sequencing the full length of the *folA* gene insert of the pET15b vector using T7 forward and reverse primers. Sequencing was done at either the Recombinant DNA/Protein Resource Facility of Oklahoma State University (Stillwater, OK) or at the Oklahoma Medical Research Foundation (OMRF, Oklahoma City, OK).

Large scale protein expression of recombinant mutant DHFR

Transformation

High Efficiency BL21(DE3)pLysS competent cells (Promega) were transformed with 10 ng plasmid DNA of successful mutants as well as with the recombinant wild type DHFR as described under Section 2.4.1 above. For each transformation reaction 100 µl was plated undiluted on LB Agar containing 100µg/ml carbenicillin and 34µg/ml chloramphenicol. Plates were incubated overnight at 37°C.

Overnight cell growth and IPTG induction

For each mutant and the recombinant wild type a single colony was grown overnight in 10 ml LB-Broth with 100 µg/ml carbenicillin and 34µg/ml

chloramphenicol in a shaking incubator at 37°C and 225 rpm. Cells were then centrifuged at maximum speed (2135 x g) at 4°C for 10 minutes (Sorval RTH-250 rotor) and resuspended in 10 ml fresh LB-medium with 100 µg/ml carbenicillin and 34µg/ml chloramphenicol. Each overnight culture was used to inoculate 500 ml LB medium containing 100 µg/ml carbenicillin and 34µg/ml chloramphenicol. Cultures were grown in 2 L flasks in a shaking incubator at 225 rpm and 37°C until an OD600 of 0.5 – 0.7. At this point cultures were cooled down to room temperature before 0.1 M (final conc.) IPTG was added to each culture. The cultures were then grown at 28°C in a shaking incubator at 225 rpm for 24 hours. Cells were harvested by centrifugation in pre-weighed 250 ml cups at 16 000xg and 4°C for 20 minutes (Beckmann JLA 16.250 rotor). After determining the wet weight of the pellets, pellets were stored frozen at -80°C overnight.

BugBuster protein extraction

BugBuster Protein Extraction Reagent Kit, Benzonase nuclease (Novagen) and Protease Inhibitor cocktail III (Calbiochem) were used to lyse the cells and extract the soluble protein from the pellets. Pellets were resuspended in 5ml/g wet cells Bugbuster® Protein Extraction Reagent and 1 µl/ml Benzonase Nuclease reagent, 10 µl/ml proteinase cocktail and 2µl/ml lysozome (10mg/ml) and incubated on a shaker (low setting) at room temperature for 30 minutes. The cell lysate was centrifuged at 4° and 16,000 x g for 20 minutes. The supernatant was collected and first filtered

through a 0.45µ membrane filter, then through a 0.22µ membrane filter. Sterile glycerol was added to 10% and the filtrate was stored at -80°C as PreColumn samples until used. Aliquots were taken for protein determination and SDS- PAGE.

BioRAD protein determination (microassay procedure for microplates)

IgG protein standards (BioRAD) were diluted to 1.37mg/ml with sterile deionized H_2O and aliquots were kept at -80°C as stock solution. A working solution was prepared by diluting the stock solution tenfold to 0.137mg/ml. Aliquots were kept at -20°C.

For the protein assay, 550µl each of 10, 35, 50, 65 and 80µg/ml standards were prepared by appropriate dilution with sterile deionized H_2O. Each standard was loaded in triplicate on a microtiter plate.

Dilutions, varying from 1:10 – 1:3,000, were prepared with sterile deionized H_2O for each of the cell extracts. Each of these samples was also loaded in triplicate in the same microtiter plate as the standards. Sterile deionized H_2O was loaded in triplicate as an assay reagent blank. Into each well of the microtiter plate with protein and blank, 40µl BioRAD dye reagent concentrate was added. The microplate was shaken on a plate shaker at medium speed for 20 – 30 minutes and absorbance was determined at 595 nm in a microplate reader (microplate auto reader EL311, BIO-TEK Instruments).

Polyacrylamide gel electrophoresis (SDS-PAGE)

For each extract samples were prepared and electrophoresis performed as described above.

Purification of recombinant mutant and wild type DHFR (semi-automated procedure)

The target protein was purified using His-Bind resin (Novagen) under non-denaturing conditions. According to the manufacturer, 5.0 ml His-Resin slurry (2.5 ml settled resin) will bind about 20 mg His-tagged protein. Procedures for preparing the His-resin and Column were done according to Novagen Technical Bulletin TB054.

His-Resin and column preparation (manual operation)

Based on the amount of total protein in the Bugbuster extract, an appropriate amount of His-Resin slurry was transferred (wide mouth pipet) into either a 10 or 20 cm Econo- Column (Bio-RAD) with an inner diameter of 1.0 cm. The stop-cock at the bottom of the column was kept open in order to allow excess buffer to drain and the resin to pack. The stop-cock was closed when the buffer had reached the surface of the settled resin.

i. The following sequence was used to wash charge and equilibrate the resin:
ii. In order to wash out residual ethanol of the storage buffer, 3 column volumes of sterile deionized H_20 was loaded onto the column and allowed to drain by gravity flow.

iii. The Column was then charged by loading 5 column volumes of 1X Charge Buffer (Novagen) [1X Charge Buffer: 50 mM $NiS0_4$] (gravity flow). iii) 3 column volumes of lX Binding Buffer [5 mM imidazol, 500 mM NaCl, 20 mM Tris-HCl, pH 7.9] (Novagen) was used to equilibrate the resin (gravity flow).

Loading and washing the column (manual operation)

The recombinant protein extract was loaded with a pipette onto the charged resin and allowed to flow by gravity. The stop-cock at the bottom of the column was adjusted to allow for a flow rate of 12 drops per minute. The flow-through fraction was collected and saved. When all of the extract had passed through the column so that it reached the surface of the resin, the resin was washed with 10 column volumes of 1X Binding buffer that contained 5% glycerol (wash 1). The process was either repeated 2 more times (washes 2 and 3), or depending on the total amount of protein loaded, wash 3 was modified by increasing he amount of imidazol in the buffer to 40 mM. The column was then washed again with IX Binding Buffer. All washes were collected and saved. A 280 nm reading was taken of the flow-through and all the washes. Washing was continued until the 280nm reading became negligible.

Biologic LP chromatography system (BioRAD)

Before elution of the HisResin bound His-tagged recombinant DHFR with the Biologic LP chromatography system, the instrument was prepared according to the manufacturer's instructions. The lines were primed with

buffer A [5 mM imidazol, 500 mM NaCl, 20 mM Tris-HCl, pH 7.9] and Buffer B [500 mM imidazol, 500 mM NaCl, 20 mM Tris-HCl, pH 7.9] and the UV absorbance was zeroed. The system was also programmed for the elution and fractious collection steps. A BioFrac fraction collector (Bio-RAD) was connected to the chromatography system and was controlled automatically via the system's control unit. The elution was monitored on a connected computer using the system's LP Data View v1.01 software (Bio-RAD).

Elution (automated procedure)

The column was connected to the Biologic LP Chromatography System and the automated procedure started. The column was first washed with 5 ml of Buffer A [5 mM imidazol, 500 mM NaCl, 20 mM Tris-HCl, pH 7.9]] at a flow rate of 1ml/minute. The fraction collector was set to collect all 5 ml as one fraction. Elution was continued as a linear gradient of 0 – 100% Buffer B (5 - 500 mM imidazol) over a volume of 20 ml. The fraction collector was set to collect all with 2 ml fraction size. Elution was continued with an additional 20 ml of 100% Buffer B (500 mM imidazol) to ensure that all protein was eluted from the column. All fractions were collected with a fraction size of 2 ml.

After elution was completed (UV absorbance had reached baseline), samples were removed and aliquoted for protein determination, SDS-PAGE and enzyme assays. Samples for protein determination and SDS-

PAGE were stored at -20°C while samples for enzyme assay were stored at -80°C.

Functionality of recombinant mutant DHFR

The functionality of the mutants was determined in a standard DHFR enzyme assay in comparison to the recombinant wild type and by their ability or inability to restore growth of a DHFR-deficient *E. coli* strain (growth complementation), also in comparison to the recombinant wild type.

DHFR standard enzyme assay

The enzyme assay for determining functionality of the DHFR mutants was performed as described by Zywno-van Ginkel *et al.* (69).The 1 ml enzyme reaction mixture contained 10 mM 2-mercatoethanol (Bio-RAD), 0.1 mM NADPH – tetrasodium salt (Sigma, St. Louis, MO), 50 mM potassium phosphate – 1 mM EDTA (Promega, Madison, WI), pH 7.0 and 10 µl of the enzyme fraction. The reaction mixture was incubated at 30ºC for 3 minutes, after which 0.1 mM dihydrofolic acid (FAH_2) (Sigma) was added to initiate the reaction. The activity was measured as a decrease at 340 nm in a Spectronic Genesis 5 spectrophotometer for 3 minutes in kinetic mode with 10 second reading intervals. The enzyme fraction was appropriately diluted with BSA in order to achieve a linear reaction progress (progress curve) over the entire 3 minute period. Each enzyme sample was measured multiple times. The reaction was corrected for NADPH oxidation, by repeating the above reaction set up and incubation, but without addition of FAH_2 for the 340 nm reading. One unit was defined as the amount of

enzyme which reduced 1 μmole FAH_2 per minute based on a molar extinction coefficient of 12300 $M^{-1}cm^{-1}$ at 340 nm (26).

Kinetic assay

In order to determine the kinetic parameters of the wild type and mutant DHFR, the assay resembled the standard assay above, but with the following modifications:

For FAH_2, the NADPH concentration was kept constant at 100 μM, while the concentration of FAH_2 was varied from 5 – 0.35 μM. The 1 ml reaction was incubated for one minute as described above, but with the NADPH and the FAH_2. The reaction was initiated by addition of the enzyme and the activity was measured as described above, but for one minute at 10 second reading intervals. The amount of enzyme used was the amount that gave a linear progress curve over the 3 minute measurement during the standard assay.

For NADPH, the concentration of FAH_2 was kept constant at 100 μM, while that of NADPH was varied from 10 – 0.7 μM. The reaction components were incubated as described above and the reaction was also enzyme initiated.

IC_{50} determination

Stock solutions for each drug were prepared at 10.24mg/ml in sterile DMSO (Sigma, St. Louis, MO) and stored at -20°C. For the drug assay the stock solution was diluted with sterile DMSO to 1.024mg/ml. This

working solution was used to prepare a series of drug concentrations ranging from 1024 µg/ml to 0.01024µg/ml.

The assay resembled the standard enzyme assay as described above. At first the standard assay was done in order to determine the amount of enzyme to be used throughout the assay. The 1 ml enzyme reaction mixture contained 10 mM 2-mercatoethanol (Bio-RAD), 50 mM potassium phosphate – 1 mM EDTA (Promega, Madison, WI), pH 7.0 and 0.1 mM NADPH – tetrasodium salt (Sigma, St. Louis, MO) as well as 10 µl of the enzyme fraction and the appropriate drug concentration respectively. The reaction mixture was incubated at 30ºC for 3 minutes, after which 0.1 mM dihydrofolic acid (FAH_2) (Sigma) was added to initiate the reaction. The activity was measured as a decrease at 340 nm in a Spectronic Genesis 5 spectrophotometer for 3 minutes in kinetic mode with 10 second reading intervals. In order to determine the effect of DMSO on the reaction, the reaction set up was repeated with 10 µl of DMSO only, instead of the drug. The effect of NADPH oxidation was taken into account as described under the standard assay. Percentage inhibition was calculated by determining the quotient of the activity obtained with the drug and that obtained in the reaction with DMSO only. At least 4 values were determined for each enzyme sample: 2 above the 50% inhibition and 2 below. The concentration of the drug that inhibited the reaction by 50% (IC_{50}) was computed using the 4 parameter curve program of the KC junior software (Bio-TEK, Winooski, VT).

Growth complementation

The DHFR-deficient strain *MG1655folA::kan3* as well, as its parent strain MG1655, (25), was available in our laboratory as frozen glycerol stocks. A sterile inoculation loop was used to transfer and streak out some cells from these frozen glycerol stocks onto LB-Agar. The LB-Agar for the parent strain did not contain any antibiotics, while that of the DHFR-deficient strain contained 30 μg/ml kanamycin (GIBCO™/Invitrogen) and 50 μg/ml thymidine (Sigma). The plates were incubated overnight at 37ºC (Isotemp incubator, Fischer Scientific).

For each strain an isolated colony was selected and grown overnight in 12.5 ml LB-medium that contained no antibiotics for the parent strain, but 30 μg/ml kanamycin and 50 μg/ml thymidine for the DHFR-deficient strain.

The 12.5 ml overnight cultures were used to inoculate 250 ml LB-medium respectively that contained the same antibiotic conditions as before. The cultures were grown at 37ºC in a shaking incubator at 225 rpm until an OD600 of 0.5-1.0 (approximately 6 hours). Cells were then chilled on ice for 15 – 30 minutes and centrifuged at 4ºC for 15 minutes at 4,000xg. The pellets were suspended in 250 ml sterile H_2O and re-centrifuged as above. These pellets were resuspended in 125 ml sterile H_2O and centrifuged as above.

The pellets were resuspended in 5 ml 10% glycerol. After centrifugation as above, the pellets were resuspended in 500 μl 10% glycerol, aliquoted into sterile eppendorf tubes and stored at -80ºC.

Electro Transformation

MGl655*folA::kan3* cells prepared above were thawed on ice and 80 µl cells were transferred to each of 10 sterile microcentrifuge tubes. To each tube 10 ng of DNA were added according to the schedule below (Table 7)

Table 7**.** Reaction set up for electro transformation of MG1655*folA::kan3* cells with plasmid DNA of the recombinant wild type and mutant *M. avium* DHFR**.**

Cells	Plasmid DNA
MG1655*folA::kan3*	no DNA added
MG1655*folA::kan3*	p807 recombinant wild type DHFR
MG1655*folA::kan3*	D31A mutation
MG1655*folA::kan3*	D31E mutation
MG1655*folA::kan3*	D31Q mutation
MG1655*folA::kan3*	D31N mutation
MG1655*folA::kan3*	D31L mutation
MG1655*folA::kan3*	V76A mutation
MG1655*folA::kan3*	pET15b vector only
MG1655*folA::kan3*	Vector pGEM11z(f) + only

It was necessary for the DNA to be very clean, (i.e. no salt) in order for the gene pulser apparatus not to arc. Tubes were allowed to sit on ice for 1 minute. The gene pulser apparatus were set 25 µF and 2.5kV.

The pulse controller was set at 200Ω.

The cell /DNA mixture was transferred to chilled 0.2 cm electroporation cuvettes (BioRad) and tapped gently to remove any bubbles. Cuvettes were placed in the chamber slide and pushed into the chamber, until the curette was seated between the contacts in the base of chamber, and pulsed once at the above settings. The time constant were recorded. The cuvettes were then removed and 1 ml SOC medium (Invitrogen) was added immediately to the cuvettes. The cells were then transferred to a sterile micro centrifuge tube or a small sterile snap cap tube and incubated for 1 hour at 37ºC and 225 rpm (rotary aeration). For each reaction, 100 µl was plated on LB-Agar, containing 30 µg/ml kanamycin, 50 µg/ml thymidine and 100 µg/ml carbenicillin. The plates were incubated overnight at 37ºC (Isotemp incubator, Fischer Scientific). An isolated colony was selected and grown overnight in 12.5ml LB-medium containing 30 µg/ml kanamycin, 50 µg/ml thymidine and 100 µg/ml carbenicillin.

Growth assay with thymidine

The overnight culture was used (~ 50 µl) to inoculate 30 ml LB-medium (30 µg /ml kanamycin, 50 µg/ml thymidine and 100 µg/ml carbenicillin) to achieve an OD600 of 0.008 – 0.011. This set up culture was further diluted as follows: 25 ml was combined with additional 25 ml fresh LB-medium containing 30 µg/ml kanamycin, 50 µg/ml thymidine and 100 µg/ml carbenicillin (1:1 dilution) in 125 ml

sterile flasks. An OD600 reading was taken for the time point t=0. This sample was serially diluted (10^{-1} – 10^{-7}) with sterile H_2O and 10 µl of each dilution plated on LB-Agar with the same antibiotic conditions as above. The cultures were grown at 37ºC and 225 rpm. Samples were taken after 2, 4, 6 and 8 hours. For each interval an OD600 reading was taken and samples were serially diluted as plated on LB-agar (see above). The agar plates were incubated at 37ºC (Isotemp incubator, Fischer Scientific) overnight (about 15 hours) and plates were used to determine CFUs. A growth curve was constructed by plotting CFU/ml against time.

Growth assay without thymidine

Freshly transformed cells that were grown overnight on LB-agar with thymidine, were used to streak LB-agar that contained 30 µg/ml kanamycin and 100 µg/ml carbenicillin, but no thymidine. It was necessary to add IPTG to a final concentration of 0.1 mM to the growth medium that did not contain thymidine. The same procedure was followed as described above in the growth assay with thymidine. A growth curve was also constructed by plotting CFU/ml against time.

Circular dichroism

Circular dichroism spectra were obtained at 25ºC with a Jasco-715 spectropolarimeter using a 0.1-cm path length cell over the 195-260 nm range. The spectra were acquired every 1 nm with a 2-s averaging time per point and a 1-nm band pass. Quadruplicate measurements of each sample were averaged, corrected for background and smoothed. The proteins were dissolved in 20 mM

sodium phosphate, 100mM NaCl, pH 7.4 and the protein concentration was determined by UV absorption spectroscopy using an extinction coefficient, at 280nm, of 39,500 $M^{-1}cm^{-1}$. The mean residue ellipticity (MRE in $deg.cm^2.dmol^{-1}$) was calculated from the number of residues of the recombinant DHFR. The secondary structure of the proteins, including regular and distorted α-helix, regular and distorted β-sheet, turns, and unordered structures, was estimated with according to Sreerama *et al*. ((56), with the program SELCON3 using a 29-protein data set of basic spectra.

CHAPTER III

RESULTS

Mutagenesis

Sequencing data showed that the GeneEditor (Promega) mutagenesis protocol used to construct the *M. avium* DHFR mutants used in this study was not only successful, but highly efficient. Efficiencies of 80% and higher were achieved. This shows the considerable improvement of mutagenesis protocols as routine research tools when compared to mutagenesis studies done in the 1980s. Then efficiencies were between 5 and 30% (54, 64, 68). For their mutagenesis experiments of aspartic acid 27 in *E. coli*, Villafranca *et al.* (64) achieved a mutagenesis efficiency of only 0.3%.

The far-UV CD spectra of recombinant wild type *M. avium* DHFR and the mutations D31A, D31E, D31Q, D31N, D31L and L32D are shown in Figure 7. Consistent with the α/β sheet motif, the spectra of the proteins show a minimum at 215nm and becomes positive below 200 nm. The estimates of the four structural components (α-helix, β-sheet, β-turns and unordered) are listed in Table 16. Three of the mutants (D31A, D31E and L32D) have CD spectra (Panel A-Fig 7), and deduced secondary structure (Table 16), which are nearly identical to the spectrum of the wild type *M. avium* DHFR. However, the spectra of the D31L, D31N and D31Q mutations show differences with the spectra of the wild type protein. Replacement of D31 by leucine, asparagine and glutamine appears to have resulted in a reduction of the β-sheet content of the mutant enzymes.

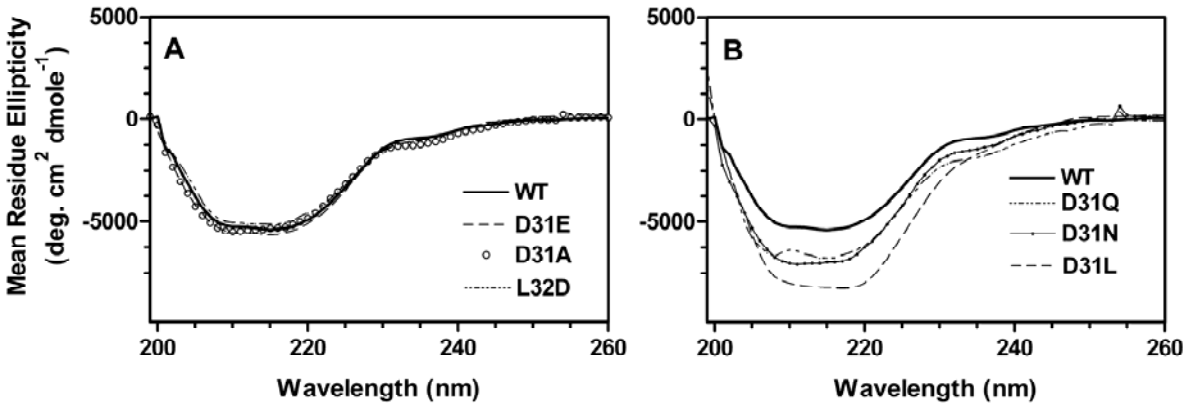

Figure 7:Far-UV CD spectra of recombinant wild type and mutant *M. avium* DHFR. Spectra were acquired in 20mM sodium phosphate, 100mM NaCl, pH 7.4 and 25 °C. For clarity the spectra are represented in two panels. With exception of the spectrum for the L32D mutant, which was obtained from a single protein sample, the spectra shown represent the average obtained from at least two independent protein preparations. Protein names and corresponding symbols are indicated in the figure.

Protein expression and purification

Sufficient amounts of soluble recombinant mutant proteins (at least 50% or higher) were obtained from expression in *E. coli* BL21(DE3)pLysS cells.

His-Bind resin (Novagen) was used to recover recombinant wild type and mutant *M. avium* DHFR from the soluble fraction of a cell extract under non-denaturing conditions. In this semi-automated process, His-Bind resin columns were loaded and washed manually and by gravity flow until the flow through showed no significant reading at 280 nm. The automated elution of the His-Bind resin bound protein with a 5 – 500 mM imidazol linear gradient is shown in Figure 8 for the recombinant wild type DHFR.

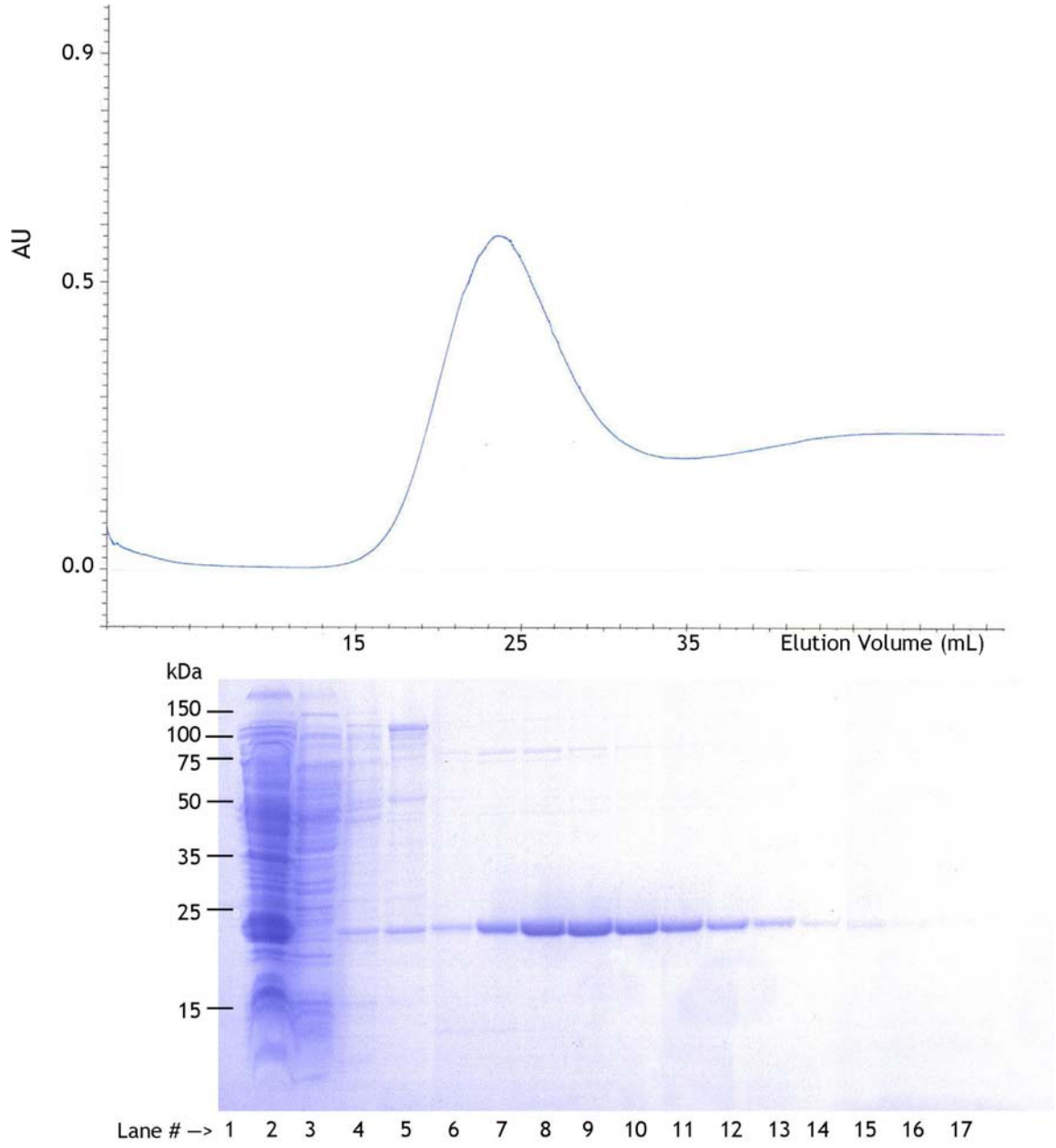

Figure 8**:**Semi-automated purification scheme of recombinant wild type DHFR on His-Bind resin (Novagen) with a linear gradient of 5-500 mM imidazol

A. UV absorbance profile of Biologic LP UV monitor (BioRAD) of elution
B. Coomassie-blue stained SDS-PAGE gel (12.5% Tis-HCl) of His-Bind resin eluted fractions

Lane 1: Novagen Perfect Protein Markers (kDa sizes indicated on the left)
Lane 2: Precolumn protein extract
Lane 3: Flow through
Lane 4: Wash 5 mM imisazol
Lane 5: Wash 40 mM imidazolLane 6-17: Eluted fractions 9- 20

The flow through fraction (Figure 8B, lane 3) shows that most DHFR bound to the His-Bind resin. There is almost no DHFR band visible in the flow through fraction. However, the low imidazol fractions (5 and 40 mM) in lanes 4 and 5 indicate that some of the binding to the His-Bind resin was non-specific. The bound protein eluted between 150 and 300 mM imidazol, with the peak of the elution profile being around 300 mM imidazol (Figure 8A). The elution profile for the recombinant wild type and mutant DHFR were very consistent and similar. Table 8 shows the amount of active enzyme recovered as well as the overall yield in purified DHFR. The percentage yield of sufficiently clean active enzyme in this case was 33.7%. This corresponds to an increase in fold purification of between 10 and 14 times.

Table 8 Semi-automated purification of recombinant wild type DHFR on His-Bind resin (Novagen) with a linear gradient of 5-500 mM imidazol

Fraction	Fraction Volume	Protein conc.mg/ml	ΔA340	Total Activity	Total Protein	Specific Activity	Yield	Fold Purification
	ml	mg/ml	µmole/min/ml	µmole/min	mg	µmole/min/mg	%	
PreColumn Extract	10.0	44.0	47.6	767	7042.78	1.08	100	--
E10	2.0 ml	1.39	12.9	25.8	2.78	10.4	3.39	9.63
E11	2.0 ml	2.33	29.3	58.6	4.66	12.6	7.69	11.7
E12	2.0 ml	2.4	31.7	63.4	4.80	13.2	8.33	12.2
E13	2.0 ml	2.05	27.6	55.2	4.10	13.5	7.25	12.5
E14	2.0 ml	1.46	15.5	31.0	2.92	10.6	4.07	9.82
E15	2.0 ml	0.618	6.67	13.3	1.24	10.7	1.75	9.91
E16	2.0 ml	0.301	4.63	9.26	0.602	15.4	1.22	14.3
Totals							33.7	

Aspartic acid 31 mutations

Specific activity

His-Bind resin eluted fractions were assayed for enzyme activity in an *in vitro* enzyme assay and the results show a significant reduction in enzyme specific activity for all the D31 mutants assayed. (D31A, D31E, D31Q, D31N and D31L). Tables 9 and 10 below show that although these recombinant mutant *M. avium* DHFRs still display functionality, the activity is significantly reduced. D31A and D31L show a reduction in enzyme activity of over 90% while D31E, D31Q and D31N show a reduction of 81.1%, 85.3% and 84.6%, respectively as compared to the recombinant wild-type *M. avium* DHFR. However, the negative control mutation V76A did not show a reduction in activity compared to the recombinant wild type.

Using the SAS statistical software (SAS system for Windows V8, SAS Inst. Inc, NC, USA), the Dunnett's Test shows (at significance level alpha = 0.05) that with the exception of the control mutation V76A, the enzyme specific activity of all D31mutations are significantly different from that of the recombinant wild type p807 (Table 9).

The control mutation V76A outside the enzyme's active site still has a specific activity that amounts to 98.7% of that of the recombinant wild type and is therefore statistically not different from the wild type.

Table 9.Comparison of enzyme specific activity (μmole min^{-1} mg^{-1}) of D31 mutated (D31A, D31E, D31Q, D31N, D31L) and control mutant (V76A) DHFR to that of the recombinant wild type (p807) at pH 7.0 and 30°C using the ANOVA and Dunnett procedures in the SAS statistical software (SAS system for Windows V8, SAS Inst. Inc, NC, USA) Dunnett significance level $\alpha = 0.05$

DHFR	Specific Activity μmole min^{-1} mg^{-1}	% relative specific activity	% decrease in specific activity over wild type	Dunnett Alpha=0.05
p807	15.4	100	==	==
D31A	1.05	6.82	93.2	$P < 0.0001$
D31E	2.91	18.9	81.1	$P < 0.0001$
D31Q	2.26	14.7	85.3	$P < 0.0001$
D31N	2.37	15.4	84.6	$P < 0.0001$
D31L	0.060	0.39	99.6	$P < 0.0001$
V76A	15.2	98.7	1.30	$P = 0.914$

In a multiple comparison, also using the SAS statistical software, the TUKEY post-test shows, that although all the D31 mutants are significantly different from the recombinant wild type in their specific enzyme activity, they are not all significantly different among themselves (Table 10A).

Table 10B shows that there are 3 groups, where DHFRs with the same group letter are not significantly different from each other, but significantly different to DHFRs in the other groups.

Table 10.Multiple comparison of enzyme specific activity (μmole min^{-1} mg^{-1})of recombinant wild type (p807) and D31mutated (D31A, D31E, D31Q, D31N, D31L) as well as control (V76A) DHFR at pH 7.0 and 30°C using the ANOVA and TUKEY procedures in the SAS statistical software (SAS system for Windows V8, SAS Inst. Inc, NC, USA) . TUKEY significance level α = 0.05.

A. Individual comparison with *P*-value.

B. Mutants without significant differences appear in the same row (same group letter), while mutants with significant differences appear in different rows (different group letters)

A

mutations compared		***P* value**	**mutations compared**		***P* value**
D31A	D31E	< 0.0001	D31L	D31N	< 0.0001
D31A	D31L	< 0.0001	D31L	D31Q	< 0.0001
D31A	D31N	< 0.0001	D31L	p807	< 0.0001
D31A	D31Q	< 0.0001	D31L	V76A	< 0.0001
D31A	P807	< 0.0001	D31N	D31Q	0.924
D31A	V76A	< 0.0001	D31N	p807	< 0.0001
D31E	D31L	< 0.0001	D31N	V76A	< 0.0001
D31E	D31N	0.252	D31Q	p807	< 0.0001
D31E	D31Q	0.169	D31Q	V76A	< 0.0001
D31E	p807	< 0.0001	p807	V76A	1
D31E	V76A	< 0.0001			

B

GROUP	DHFR							
A	P807	V76A						
B			D31E	D31N	D31Q			
C							D31A	D31L

Kinetic characteristics of D31 mutant DHFR

The kinetic parameters K_m and V_{max} for FAH_2 and NADPH of the recombinant wild type *M. avium* DHFR (p807) and its D31mutants were determined using the non-linear Michaelis-Menten curve fitting program Enzfitter (Biosoft, UK) (Figure 9) and are listed in Table 11. The D31A and D31L mutants show the greatest changes in kinetic characteristics compared to the recombinant wild type (p807). The $K_m(FAH_2)$ is 37 μM for D31A and 198μM for D31L compared to the 0.70 μM for p807. This corresponds to a 51-fold increase for D31A and a 283-fold increase for D31L.

The $K_m(FAH_2)$ for D31E, D31Q and D31N is 1.92, 2.32 and 2.08 μM, respectively; a moderate increase of between 2 and 2.5-fold over p807. On the other hand D31Q and D31N show a slight decrease in their K_m(NADPH): 0.65 and 0.77 μM, respectively. With a K_m of 2.01 μM, D31E shows a slight increase in K_m(NADPH) over the recombinant wild type. In contrast to its $K_m(FAH_2)$ that showed a 283-fold increase, the K_m(NADPH) value of 1.44 μM of the D31L mutant is not very much different from that of the recombinant wild type. The D31A, D31Q and D31L mutants had the lowest $k_{cat}/K_m(FAH_2)$ values: 2.30×10^4, 6.50×10^5 and 1.26×10^2, $s^{-1}M^{-1}$ respectively, while D31E and D31N were very similar with 1.87×10^6 and 2.4×10^6 $s^{-1}M^{-1}$, respectively (Table 11).

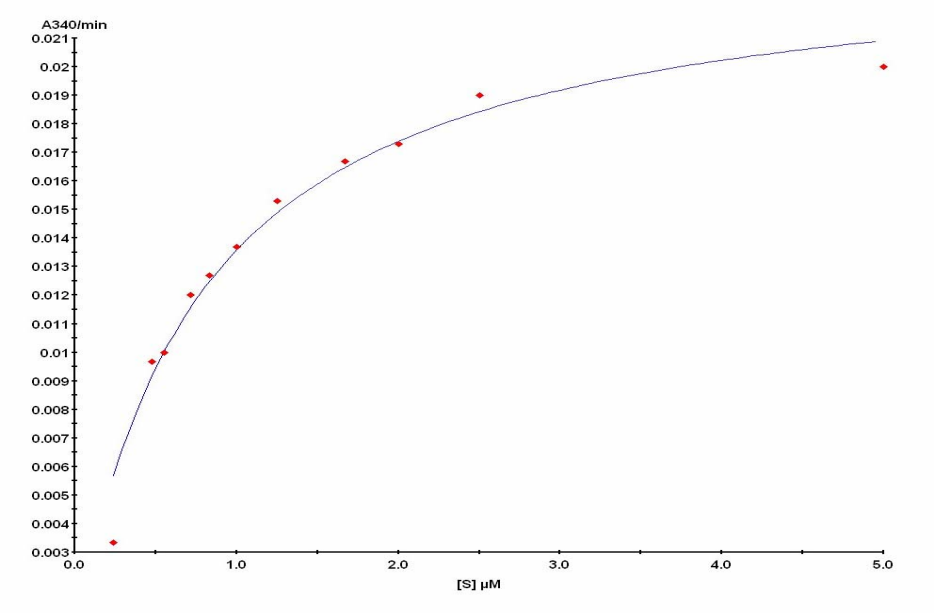

Figure 9:Determination of Michaelis-Menten parameters $K_m(FAH_2)$ and $V_{max}(FAH_2)$ of recombinant wild type *M. avium* DHFR (p807) at pH 7.0 and 30°C using the non-linear curve fit program Enzfitter (Biosoft, UK). Reaction was initiated by addition of enzyme after the substrates dihydrofolate and NADPH were incubated at 30°C for 1 minute. Absorbance was measured at 340 nm for minute in a Spectronic Genesis 5 spectrophotometer in kinetic mode with 10 second reading intervals.

K_m(NADPH) for the D31A mutant was with 0.68 µM similar to that of the mutants D31Q and D31N. The data indicate that the control mutation V76A did not affect the K_m for both FAH_2 and NADPH. This mutant had a $K_m(FAH_2)$ of 0.78 µM compared to 0.7 µM of the recombinant wild type. The K_m(NADPH) of the V76A control mutant was 1.56 µM compared to 1.55 µM of the recombinant wild type.

For both substrates there was more variation in V_{max} among the D31 mutants, than there was in K_m. The V_{max}(NADPH) of the V76A control mutant was the only one that was not much different from the recombinant wild type.

The data indicate that the control mutation V76A did not affect the K_m for both FAH_2 and NADPH (Table 11).

Table 11**:**Kinetic parameters at pH 7.0 and 30°C of recombinant wild type and D31mutants of *M. avium* DHFR for FAH_2 and NADPH determined with the non-linear Michaelis-Menten curve fitting program Enzfitter (BioSoft, UK).

	FAH_2				NADPH	
DHFR	K_m	V_{max}	k_{cat}	k_{cat}/K_m	K_m	V_{max}
	(μM)	μmole min^{-1} mg^{-1}	sec^{-1}	s^{-1} M^{-1}	(μM)	μmole min^{-1} mg^{-1}
p807	0.7	61.1	20.5	$2.90x10^7$	1.55	80
D31A	37	2.57	0.86	$2.30x+10^4$	0.68	1.76
D31E	1.92	10.7	3.58	$1.87x10^6$	2.01	6.16
D31Q	2.32	4.51	1.5	$6.5010x^5$	0.65	6.53
D31N	2.08	15.1	5.03	$2.40x10^6$	0.77	25.5
D31L	198	0.076	0.025	$1.26x10^2$	1.44	0.06
V76A	0.78	56.4	18.7	$2.40x10^7$	1.56	71.3

Growth complementation

The DHFR-deficient *E. coli* strain MG1655*folA::kan3* ($folA^-$) was transformed with plasmid DNA of the recombinant wild type *M. avium* DHFR (*folA*-p807), as well as that of the aspartic acid 31 mutants (*folA*-D31A, *folA*-D31E, *folA*-D31Q, *folA*-D31N, *folA*-D31L) and the mutation control V76A (*folA*-V76A). In addition, the DHFR-deficient strain was also transformed with plasmid DNA of the pET15b vector that did not contain the *M. avium* DHFR gene insert (*folA*-pET15b).

Figure 10A below shows that all cells show similar and normal growth, comparable to that of the parent strain MG1655, when grown in the presence of thymidine.

When, however, the DHFR-deficient strain transformed with plasmid DNA that carried the *M. avium* DHFR gene (recombinant wild type p807) as well as the various D31 mutations, respectively, was cultured in the absence of thymidine, only the wild type (p807) and the control mutation V76A showed growth of the DHFR-deficient strain to levels comparable to that of the *E. coli* MG1655 parent strain (Figure 7B). Neither the DHFR-deficient *E. coli* MG1655*folA::kan3 (folA*$^{-}$) strain nor any of the D31 mutants showed any significant growth. The DHFR-deficient strain that was transformed with the pET15b Vector that did not contain the *M. avium* DHFR gene also did not show any growth (Figure 10B).

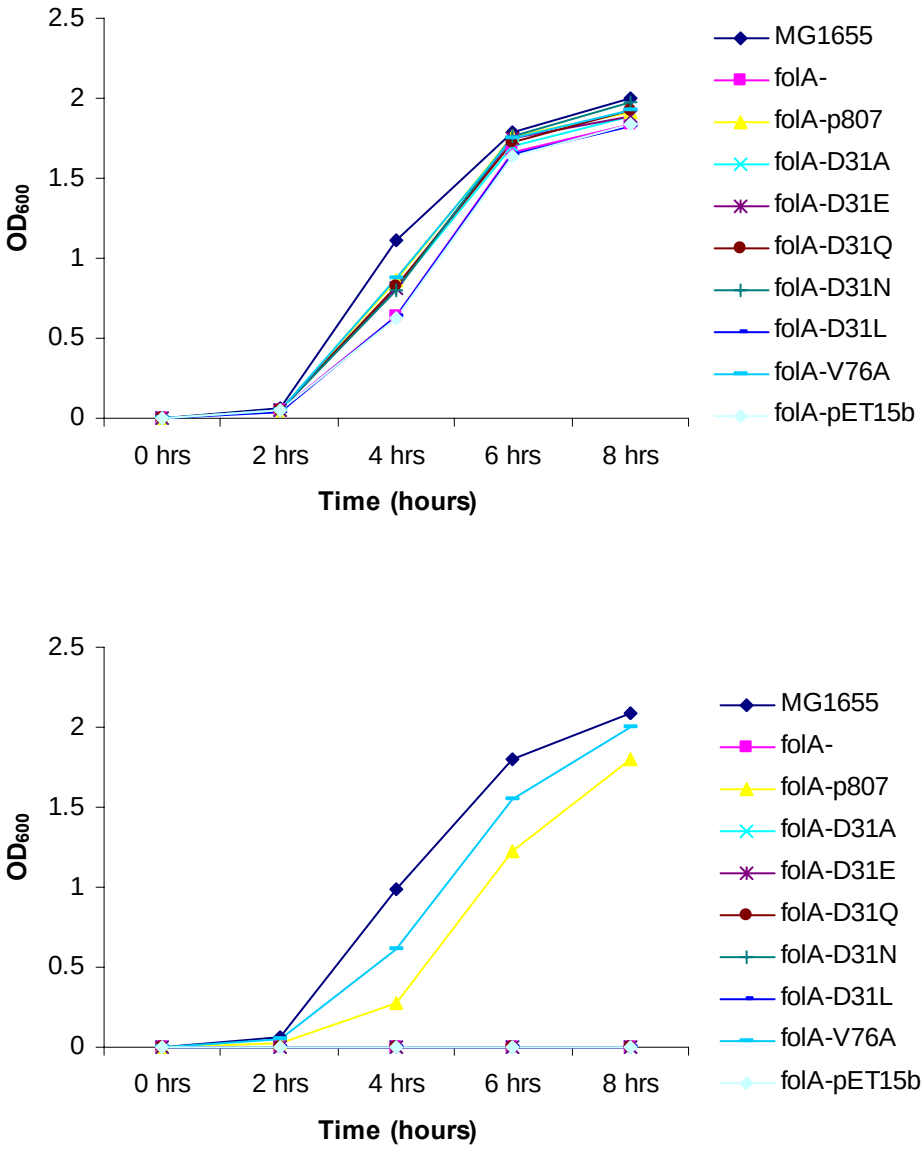

Figure 10**:**Growth curve at 37°C and 225 rpm of DHFR-deficient *E. coli* strain MG1655*folA::kan3* transformed with recombinant wild type *M. avium* DHFR (p807), D31 mutants and the controls (V76A and pET15b vector only). Growth in the presence of thymidine **(**A**)** and growth in the absence of thymidine **(**B**)**

Leucine 32 mutations

Specific activity

In contrast to the aspartic acid 31 (D31) mutations only one of the 3 L32 mutations of *M. avium* DHFR caused a significant change in the mutant enzyme's specific activity as compared to the recombinant wild type enzyme (Table 12). Both the L32F and the L32A mutations did not have an impact on the enzyme's interaction with the substrate dihydrofolate. Compared to the recombinant wild type, the L32F mutation had a slightly higher relative specific activity (103%), showing that statistically (Dunnett's test P=0.759 at $\alpha = 0.05$) this mutation was not different from the recombinant wild type (Table 12). The L32A mutation of the *M. avium* DHFR still had 96% of the specific activity of the recombinant wild type enzyme, therefore statistically (Dunnett's test P=0.742 at $\alpha = 0.05$) not different from the recombinant wild type. The L32D mutation was the only one of the 3 mutations in this series that had a negative impact on the mutant enzyme's activity. This mutant had a 67% reduction in its specific activity as compared to the recombinant wild type and was therefore found to be statistically different from the recombinant wild type (Dunnett's test P<0.0001 at $\alpha = 0.05$).

Table 12**.** Comparison of enzyme specific activity (µmole $min^{-1}mg^{-1}$) of L32 mutated (L32F, L32A, L32D) DHFR to that of the recombinant wild type (p807) at pH 7.0 and 30°C using the ANOVA and Dunnett procedures in the SAS statistical software (SAS)system for Windows V8, SAS Inst. Inc, NC, USA) Dunnett significance level $\alpha = 0.05$

DHFR	**Specific Activity µmole $min^{-1}mg^{-1}$**	**% relative specific activity**	**% decrease in specific activity over wild type**	**Dunnett Alpha = 0.05**
p807	15.4	100	-	-
L32F	16	103	-	$P = 0.759$
L32A	14.7	96	4	$P = 0.742$
L32D	5.09	33	67	$P < 0.0001$

The Dunnett's test only compared each mutant to the wild type for differences, not the mutants among themselves. In a multiple comparison test using SAS statistical software (SAS system for Windows V8, SAS Inst. Inc, NC, USA), the TUKEY-post-test showed that the L32F and L32A mutants were not statistically different from each other (P=0.370 at $\alpha = 0.05$), but that they were each statistically different from the L32D mutations (P<0.0001 at $\alpha = 0.05$ for both cases). These results are summarized in Table 13A and B.

Table 13. Multiple comparison of enzyme specific activity (μmole $min^{-1}mg^{-1}$) of recombinant wild type (p807) and mutated (L32F, L32A, L32D) *M. avium* DHFR at pH 7.0 and 30°C using the ANOVA and TUKEY procedure in the SAS statistical software (SAS system for Windows V8, SAS Inst. Inc, NC, USA). (TUKEY significance level alpha=0.05).

A. Individual comparison with *P*-value:

B. Mutants without significant differences appear in the same row (same group letter),while mutants with significant differences appear in different rows (different group letters)

A

mutations compared		***P* value**
p807	L32F	0.85
p807	L32A	0.838
p807	L32D	<0.0001
L32F	L32A	0.37
L32F	L32D	<0.0001
L32A	L32D	<0.0001

B

GROUP	DHFR			
A	p807	L32F	L32A	
B				L32D

Kinetic characteristics of L32 mutant DHFR

The kinetic parameters K_m and V_{max} for dihydrofolate (FAH_2) and NADPH were also determined at pH 7.0 and 30°C using the non-linear Michaelis-Menten curve fitting program Enzfitter (Biosoft, UK) and are listed in Table 14 for the recombinant wild type and the L32 mutants of *M. avium* DHFR. The L32F and L32A mutants were not very different from the recombinant wild type in

$K_m(FAH_2)$ values. The $K_m(FAH_2)$ of the recombinant wild type was 0.7μM, while that of the L32F mutant was 0.68 μM. The L32A mutant had a slightly higher $K_m(FAH_2)$ of 0.96 μM. With a $K_m(FAH_2)$ of 5.12 μM, the L32D had a 7-fold increase in $K_m(FAH_2)$ over the recombinant wild type.

The mutants L32F and L32A were also not much different from the recombinant wild type in their $V_{max}(FAH_2)$ values. The recombinant wild type had a $V_{max}(FAH_2)$ of 61.1 μmole min^{-1} mg^{-1}, while the L32F and L32A mutants had a $V_{max}(FAH_2)$ of 63.3 and 55.2 μmole min^{-1} mg^{-1}, respectively. The mutant L32D had a $V_{max}(FAH_2)$ of 21.5 μmole min^{-1} mg^{-1}; a value almost 3-fold lower than the recombinant wild type (Table 14).

The L32F mutant's $k_{cat}/K_m(FAH_2)$ was just slightly higher than the recombinant wild type. The $k_{cat}/K_m(FAH_2)$ of the L32F mutant was $3.09x10^7$ $s^{-1}M^{-1}$, whereas that of the recombinant wild type was $2.90x10^7$ $s^{-1}M^{-1}$. The L32A mutant of *M. avium* DHFR had a lower $k_{cat}/K_m(FAH_2)$ compared to the recombinant wild type. With a $k_{cat}/K_m(FAH_2)$ value of $2.0x10^7$ this mutant's $k_{cat}/K_m(FAH_2)$ value was almost 1.5-fold lower than that of the recombinant wild type. On the other hand the L32D mutant had a $k_{cat}/K_m(FAH_2)$ value of $1.41x10^6$ $s^{-1}M^{-1}$ which was almost 21-fold lower than that of the recombinant wild type (Table 14).

The recombinant wild type *M. avium* DHFR and the mutants L32F and L32A were also similar with respect to NADPH binding. The recombinant wild type had a K_m(NADPH) of 1.55 μM, whereas that of the L32F and L32A mutants were 1.32 and 1.39μM, respectively. The K_m(NADPH) of the L32D mutant was 0.84 μM and therefore almost 2-fold lower than that of the recombinant wild type. The

recombinant wild type and the L32F and L32A mutants had a V_{max}(NADPH) of 80, 69.6 and 53.5 µmole min^{-1} mg^{-1}, respectively (Table 14), whereas V_{max}(NADPH) of the L32D mutant was 30.1 µmole min^{-1} mg^{-1}.

Table 14. Kinetic parameters at pH 7.0 and 30°C of recombinant wild type and L32 mutants of *M. avium* DHFR for FAH_2 and NADPH determined with the non-linear Michaelis-Menten curve fitting program Enzfitter (BioSoft, UK).

	FAH_2				NADPH	
DHFR	K_m	V_{max}	k_{cat}	k_{cat}/K_m	K_m	V_{max}
	(µM)	(µmole $min^{-1}mg^{-1}$)	sec^{-1}	s^{-1} M^{-1}	(µM)	(µmole $min^{-1}mg^{-1}$)
p807	0.7	61.1	20.5	2.90×10^7	1.55	80
L32F	0.68	63.3	21	3.09×10^7	1.32	69.6
L32D	5.12	21.5	7.2	1.41×10^6	0.84	30.1
L32A	0.96	55.2	16.2	1.69×10^7	1.39	53.5

Growth complementation

As shown in Figure 11, the L32F and L32A mutants of the *M. avium* DHFR was able to complement the DHFR-deficient strain *E. coli* MG1655*folA::kan3* and restored growth of the deficient strain to levels comparable to its parent strain *E. coli* MG1655. The DHFR-deficient strain *E. coli* MG1655*folA::kan3* grew when supplemented with thymidine (Figure 10A, *folA*$^-$*),* but did not grow in the absence of thymidine (Figure 11B, *folA*$^-$). When transformed with plasmid DNA of *M. avium* DHFR mutants L32F and L32A, the DHFR-deficient *E. coli*

MG1655*folA::kan3* strain was able to grow in the absence of thymidine, indicating that these DHFR mutants of *M. avium* was able to restore DHFR activity to *E. coli* and thereby restore growth (Figure 11B, *folA*$^-$L32F and *folA*$^-$ L32A). The L32D mutant did not restore growth of the DHFR-deficient strain to levels comparable to the E. coli parent strain MG1655, but was able to cause partial growth in the deficient strain (Figure 11B, *folA*$^-$L32D).

Inhibitor IC_{50} assay

After the appropriate amount of enzyme to be used in the IC_{50} assay was determined in the standard assay, the IC_{50} assay was performed similarly to the standard enzyme assay, with the exception that the 1 ml enzyme reaction contained both the enzyme and the inhibitor, pre-incubated in a water bath at 30°C for 3 minutes. The reaction was initiated by addition of dihydrofolate and measured in kinetic mode for 3 minutes at 340 nm.

The IC_{50} values were then computer using the 4- parameter curve program in the KC-Junior software (Bio-TEK, VT, USA). The 4-parameter curves for the recombinant wild

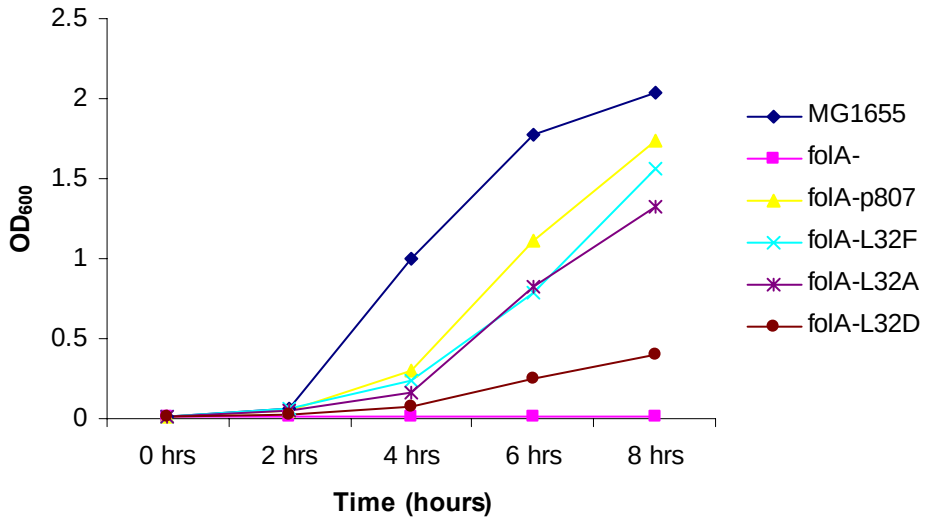

Figure 11**:**Growth curve at 37°C and 225 rpm of DHFR-deficient *E. coli* strain MG1655*folA::kan3* transformed with recombinant wild type *M. avium* DHFR (p807), L32F mutant and control pET15b vector only. Growth in the presence of thymidine (A) and growth in the absence of thymidine (B).

type, as well as the L32A and L32D mutants are displayed in Figure 12. The IC_{50} values of the recombinant wild type and the L32F mutant of *M. avium* DHFR for trimethoprim were very similar with 3869 and 3647 nM respectively. The IC_{50} value of the L32A mutant for trimethoprim, however, was with 45067 nM, about 12-fold higher than that of the recombinant wild type (Table 15). On the other hand the L32D mutant's IC_{50} value for trimethoprim was 570 nM, which was about 7-fold lower than that of the recombinant wild type.

Compared to trimethoprim, the SRI deazapteridines showed a greater selectivity for the wild type *M. avium* DHFR but that selectivity was reduced by the various L32 mutations. The IC_{50} value of the recombinant wild type for SRI compounds 8858 and 20730 were 1.03 and 1.96 nM, respectively (Table 15). The IC_{50} values of compounds 8858 and 20730 for the L32F mutant were 14.8 and 41.7 nM, respectively. Compared to trimethoprim this amounts to a reduction of 246 and

88-fold, respectively for the SRI compounds. The reduction of the IC_{50} of the L32A mutant of *M. avium* DHFR was only moderate for both SRI compounds. The L32A mutant had an IC_{50} of 507 nM for compound 8858 and 861 nM for compound 20730 (Table 15). This represents a reduction of between 52 and 88-fold between these 2 compounds when compared to trimethoprim. The reduction in the IC_{50} values of the L32D mutant for the SRI compounds were very small, between 4 and 8-fold, compared to trimethoprim. The L32D mutant had an IC_{50} of 69 nM for compound 8858 and 134 nM for compound 20730 (Table 15).

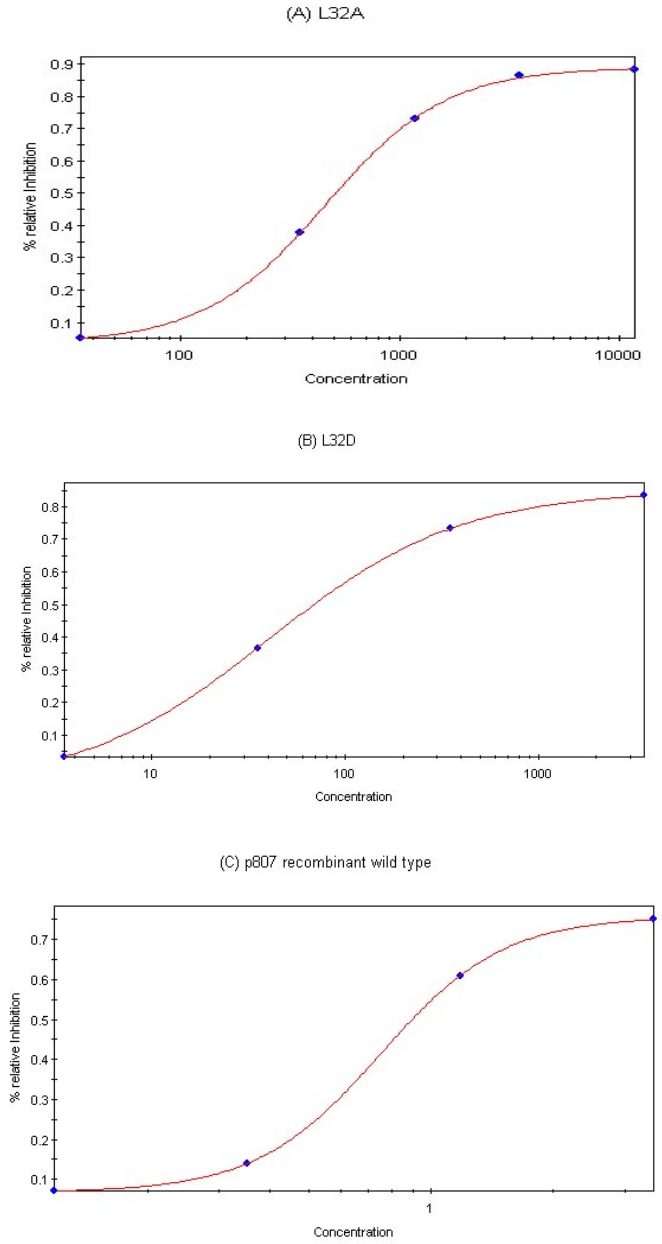

Figure 12**:** Four parameter curves for determination of IC_{50} relative concentrations of SRI compound 8858 for recombinant wild type, L32D and L32A mutants of *M. avium* DHFR.

Table 15. IC_{50} of trimethoprim (TMP) and SRI compounds 8858 and 20730 for recombinant wild type and leucine 32 mutant *M. avium* DHFR as determined by the 4 parameter curve procedure (the Bio-TEK enzyme software).

DHFR\DRUG	TMP [nM]	SRI 8858 [nM]	SRI 20730 [nM]
WT	3869	1.03	1.96
L32F	3647	14.8	41.7
L32A	45067	507	861
L32D	570	69	134

Table 16. Estimated relative amounts of secondary structural components of recombinant wild type *M. avium* DHFR and and D31 and L32 mutants. The fractions of the different structural components were calculated from the data shown in Figure 7 using the program Selcon3.

	α-helix	β-sheet	β-Turn	Unordered
WT	0.20	0.38	0.17	0.25
D31A	0.20	0.38	0.17	0.25
D31E	0.20	0.35	0.15	0.22
D31L	0.19	0.28	0.22	0.30
D31N	0.15	0.30	0.23	0.31
D31Q	0.29	0.20	0.24	0.30
L32D	0.12	0.30	0.19	0.27

CHAPTER IV

DISCUSSION

The mutagenesis procedure was highly efficient, delivering 80% and higher successful mutants as confirmed by complete gene sequencing. The control mutation V76A, which was outside the enzyme binding cavity, did not alter the enzyme's interaction with the normal substrate as compared to the recombinant wild type enzyme, thereby suggesting that the mutation process did not have a negative impact on the enzyme's proper folding. The far-UV CD spectra of recombinant wild type *M. avium* DHFR and its D31 and L32 mutants (Figure 7, Table 16) show that the inferred secondary structure of wild type *M. avium* DHFR is consistent with the crystal structures of the homologous DHFR from *M. tuberculosis* (35), and *E. coli* (10), whose structures comprise eight β strands and four α-helices. The structural information obtained by CD spectroscopy is also consistent with the homology model of *M. avium* (33) .

The use of the pET15b vector in the site-directed mutagenesis procedure, instead of the pGEM11zf(+) subcloning vector of the GeneEditor kit, circumvented multiple subcloning and excision steps. The same pET15b vector was used for cloning, mutagenesis and expression of the mutant and wild type target protein. This was possible, because essentially any plasmid vector that carries the ampicillin resistance gene could be used

with this mutagenesis kit. The pET15b vector further added an N-terminal his-tag to the expressed target protein that eventually aid in the purification of the target protein.

The expression of the recombinant target protein in *E. coli* BL21(DE3) pLysS took place at 28°C in order to minimize the expression of endogenous *E. coli* DHFR in comparison with the IPTG induced over-expression of the target protein. At least 50% of expressed target protein was recovered in the soluble protein fraction. The recovery of DHFR from the soluble extract varied from 60 – 80%, with at least half of that amount as sufficiently clean target protein (Figure 8 and Table 8).

Functionality of *M. avium* conserved aspartic acid 31 (D31) mutants

Site-directed mutagenesis has previously been used to investigate the role of this highly conserved carboxylic acid residue in catalysis and binding in *E. coli*, *L. casei* and a few other species (2, 7, 19, 29, 30, 62, 64). This is the first study that has assessed the important functional role of the conserved D31 residue in *M. avium*, or any other equivalent residue in any other mycobacterial DHFR.

All mutations of the aspartic acid 31 (D31) affected the enzyme negatively and showed a significant reduction in the enzyme's interaction with dihydrofolate, the natural substrate. The substitution D31A removed the side chain and the charge at that position altogether which resulted in a reduction of the enzyme's specific activity by almost 95%. This indicates the important functional role of this residue in *M. avium* DHFR in interacting with the normal substrate, dihydrofolate. This is also consistent with this residue's role in other DHFRs described thus far and a reflection of the strictly conserved status of this residue for all known DHFR's. (1, 3, 11, 22, 30, 34, 40, 44, 46, 60, 64). The D31E mutation that retained the important carboxylic acid group of the wild type, but is one

methylene group larger than the recombinant wild type, had its specific activity reduced by around 80%, suggesting that the larger side chain did have a negative effect on interactions within the binding cavity. The D31Q mutation which is also one methylene group larger than the recombinant wild type enzyme and has the same size as the D31E mutant, did not have the charge of the carboxylic acid group as the recombinant wild type or the D31E mutant. Nonetheless, this mutation also showed a reduction in specific activity of over 80% of the activity of the wild type; in magnitude about the same as the D31E mutation (Table 9).

The D31N and D31L mutations both have the same side chain size as the recombinant wild type's aspartic acid, however, although the D31N is not charged, it is nonetheless polar, while the D31L side chain is not charged and non-polar. With respect to side chain size and volume the D31 is almost super imposable with the mutant side chains D31N and D31L. The D31N mutant showed a reduction in specific activity of around 85% over the recombinant wild type, and therefore, behaved similarly as the D31E and D31Q mutations. The D31L mutation on the other hand had less than one percent of the specific activity of the recombinant wild type, and therefore, could be considered similar to the D31A mutation in terms of the amount of enzyme functionality displayed (Table 9). The V76A modification was a mutation outside of the enzyme's binding cavity and did not show a change in the enzyme's specific activity as compared to the recombinant wild type. This validated the mutation procedure, and therefore, it can be argued that the change in the observed reduction of the mutant enzymes' specific activity was a result of the change of the conserved aspartic acid.

Statistical analysis (ANOVA with Dunnett and Tukey) showed that all the D31 mutant enzymes in this study were significantly different from the recombinant wild type in terms of their specific activity (Table 9). However, some of the mutations were not significantly different from each other (Table 10). Although the D31E, D31Q and D31N mutations were remarkably different in terms of side chain size and charge, they were not statistically different from each other in terms of enzyme functionality. This group was distinctly and statistically different from the other mutations and the recombinant wild type (Table 10B). The D31A and D31L mutations also represent marked diversity, yet they formed another group with no significant difference in functionality between them, but statistically different from the recombinant wild type and the other mutations (Table 10B). The control mutation V76A was the only mutation that was statistically similar to the recombinant wild type in functionality and therefore together with the recombinant wild type formed a third group of enzymes that was distinctly different from the mutant enzymes (Table 10B).

Birdsall et al. (7) found that a D26E mutation in *L. casei* (the equivalent position of D31 in *M. avium*) still had 90% of the specific activity of the wild type enzyme. They also found that there were no major changes in the overall structure of the mutant enzyme. Local perturbations observed might have been necessary to accommodate the larger side chain. David et al. (18) on the other hand found that although a D27E mutant *E. coli* DHFR was still able to catalyze the reduction of dihydrofolate to tetrahydrofolate, the mutant enzyme was 17-fold less efficient than the wild type enzyme. They also did not observe any structural changes in an X-ray crystal structure of the *E. coli* D27E DHFR. The kinetic parameters of the recombinant wild type and D31 mutants of the *M. avium*

DHFR for this study are listed in Table 11. The *M. avium* DHFR D31E mutant had a $K_m(FAH_2)$ of 1.92 μM; about a 3-fold increase over the recombinant wild type, which had a $K_m(FAH_2)$ of 0.7 μM. However, the D31E mutant had a $k_{cat}(FAH_2)$ of 3.58 sec^{-1}, compared to 20.5 sec^{-1} of the recombinant wild type. Therefore, this mutant showed only a 6-fold decrease in k_{cat} (catalytic efficiency), but a 16-fold decrease in k_{cat}/k_m (substrate specificity) over the wild type (Table 11). The latter value is similar and comparable to those obtained by David *et al.* (18) for the same mutation in *E. coli*. David *et al.* (18) also pointed out that *L. casei* DHFR in certain aspects, e.g. its ability to reduce folate, resembles more DHFRs of vertebrates than that of bacteria. These differences could in part explain the differences observed with regard to the substitution of the conserved aspartic acid with glutamic acid in *M. avium, E. coli* and *L. casei. Lactobacillus casei* also has a conserved aspartic acid in this position, but vertebrates have a glutamic acid. The *M. avium* DHFR mutants D31E, D31Q and D31N in this study were very similar with $K_m(FAH_2)$ of 1.92, 2.32 and 2.08 μM, respectively (Table 11). This represents about a 3-fold increase in $K_m(FAH_2)$ over the recombinant wild type for each of these 3 mutations and reflects the strong decrease in functionality (specific activity) observed earlier (Table 9). However, these mutants showed more variations in $V_{max}(FAH_2)$ and $k_{cat}(FAH_2)$ (Table 11). With a $k_{cat}(FAH_2)$ of 5.03 sec^{-1}, D31N was more similar to D31E $k_{cat}(FAH_2)$ 3.58 sec^{-1}, than to D31Q, that had a $k_{cat}(FAH_2)$ of 1.50 sec^{-1}. The D31N and D31E mutants also had similar reductions in $k_{cat}(FAH_2)$: 4 and 6-fold respectively, was well as in $k_{cat}/K_m(FAH_2)$: a 12 and 16-fold reduction respectively. On the other hand, the D31Q mutant had a 14-fold reduction in $k_{cat}(FAH_2)$ and a 45-fold reduction in $k_{cat}/K_m(FAH_2)$. Howell et al. (30) substituted the conserved aspartic acid 27 in *E. coli*

DHFR with asparagine (D27N) and found a severely crippled enzyme. That mutant enzyme had less than 1% of the specific activity of the wild type and also severely altered kinetics (30). With a $K_m(FAH_2)$ of 44 μM and $k_{cat}(FAH_2)$ of 0.10 sec^{-1} for the *E. coli* DHFR D27N mutant (30), their values for this mutant were different from those for the same *M. avium* mutant in this study. The wild type parameters of their study were more comparable to this study. Basran *et al.* (6) investigated the role of the active site carboxylic acid D26 in *L.casei* DHFR and found that a D26N mutation in recombinant *L. casei* DHFR (equivalent position of *M. avium* D31 and *E. coli* D27) had a much smaller effect on that mutant enzyme's functionality, compared to the equivalent mutation in *E. coli* DHFR. The *L. casei* D26N DHFR had a decrease in $k_{cat}(FAH_2)$ of 9-fold, compared to 300-fold in *E. coli* and a decrease in $k_{cat}/K_m(FAH_2)$ of 13-fold compared to 11000-fold in *E. coli* (6, 30). The equivalent mutation in *M. avium* DHFR (D31N) in this study resembles more *L. casei* than *E. coli.* The *M. avium* D31N mutant DHFR had a 4-fold decrease in $k_{cat}(FAH_2)$ and a 12-fold decrease in $k_{cat}/K_m(FAH_2)$ (Table 11). Nonetheless, the overall result of these studies show that the asparagine substitution in this position affected the enzyme's activity in *E. coli, M. avium* and *L. casei*. From these mutations it is evident that with the same charge but larger side chain (D31E), and with the same size side chain but no charge (D31N), functionality of the enzyme is severely affected. Although the $K_m(FAH_2)$ of the D31Q mutation was similar to that of the D31E and D31N mutations and there was no significant difference in their specific activities, the data suggest a difference in kinetics between the D31Q on the one hand and the D31E and D31N on the other. The D31Q mutation's side chain is larger than the wild type aspartic acid residue by one methylene group (similar to the D31E mutation's side chain), and it is

not charged, but polar (similar to the D31N mutation's side chain). The combination of both adverse factors of the other two mutants (larger size and no charge as compared to the recombinant wild type aspartic acid) seem to have had an increased negative effect on the D31Q mutant enzyme's specificity for the substrate. The $k_{cat}/K_m(FAH_2)$ for D31Q had decreased by 45-fold, compared to a reduction of only 16-fold for the D31E mutant and 12-fold for the D31N mutant (Table 11). Nothing has been found in the literature for this mutation in this equivalent position on any DHFR.

The very low specific activity of the mutant D31L of the *M. avium* DHFR was also reflected in the mutants kinetic behavior. The $K_m(FAH_2)$ of this mutant was 198 μM, a 283 fold increase over the recombinant wild type. Its $k_{cat}(FAH_2)$ of 0.025 sec^{-1} was a reduction of 820-fold and the $k_{cat}/K_m(FAH_2)$ was reduced over 230, 000-fold over the recombinant wild type (Table 11). David *et al.* (18) found a D27L mutant enzyme of *E. coli* DHFR similarly dysfunctional. This mutation is identical in side chain size with the recombinant wild type aspartic acid, but has no charge and is nonpolar. It is by far the most severe change in this position of all the D31 mutants investigated, suggesting that the increased hydrophobicity had more severe negative effects than the loss of the charge alone. The D31A mutation that did not show a statistical difference in specific activity to the D31L mutation, seems to be different in its kinetic behavior from the D31L mutant. The D31A mutant had a $K_m(FAH_2)$ of 37 μM (Table 11), which represents a 53-fold increase over the recombinant wild type. The $k_{cat}(FAH_2)$ decrease over the recombinant wild type for the D31A mutation was only 24-fold, but the $k_{cat}/K_m(FAH_2)$ decrease was 1261-fold. Both the D31A and D31L were very low activity mutants with the largest increases in $K_m(FAH_2)$ over the recombinant wild type (Table 11). However, although

they did not show a statistical difference in their specific activity (Table 9 and 10A and B) and their $K_m(FAH_2)$ difference was only 5-fold, the data show a 200-fold difference between them in their $k_{cat}/K_m(FAH_2)$ values (Table 11). With the D31A mutation, the charge of the wild type carboxylic acid was removed and at the same time it had the smallest side chain of all mutants. This mutation shows that removing the carboxylic acid seriously cripples the enzyme.

The recombinant wild type and the control mutation V76A were not very different in their kinetics for both dihydrofolate and NADPH. The recombinant wild type had a $K_m(FAH_2)$ of 0.7 μM, whereas V76A had a $K_m(FAH_2)$ of 0.78 μM (Table 11). The $V_{max}(FAH_2)$ for the recombinant wild type and V76A were 61.1 and 56.4 μmole min^{-1} mg^{-1}, respectively (Table 11). The K_m(NADPH) for the recombinant wild type and V76A mutation was 1.55 and 1.56 μM, respectively, whereas V_{max}(NADPH) was 26.8 μmole min^{-1} mg^{-1} for the recombinant wild type and 23.7 μmole min^{-1} mg^{-1} for the V76A mutation. The K_m(NADPH) values of all D31 mutants were slightly reduced compared to that of the recombinant wild type. However, this reduction did not vary greatly among the D31 mutations which ranged from 0.65 to 0.77 μM, about a 2-fold reduction over the recombinant wild type. The V_{max}(NADPH) on the other hand, did show larger variation among the mutants (Table 11). Dunn *et al.* (19) as well as Appleman *et al.* (2) found that replacement of the conserved D27 in *E. coli* reduced the affinity of NADPH by 7 and 3-fold, respectively. Although this conserved aspartic acid residue is not directly involved in binding of NADPH, they argued that the increased rate of dissociation in the mutants as well as a shift in the equilibrium that favored nonbinding could be responsible for changes in affinity for NADPH. Based on the K_m(NADPH) for all D31 mutations in this

study, the effects of the mutations on NADPH seem minimal compared to that of dihydrofolate described earlier.

The functionality of the D31 mutations were overall as hypothesized. However, the extent of the reduction in activity of the D31E mutation shows the limited flexibility of *M. avium* DHFR at this position, similar to that of *E. coli* (18), but different from *L. casei* (7). The kinetic characteristics of the D31 mutations show that, with the exception of the D31A mutation, the change in $K_m(FAH_2)$ was smaller than the change in k_{cat} and k_{cat}/K_m compared to the recombinant wild type (Table 11). This suggests that the binding of the substrate to the mutant enzymes and therefore the formation of the enzyme-substrate (ES) complex is not the limiting step in the reaction. The smaller k_{cat} and even smaller k_{cat}/K_m values of the D31 mutations compared to the recombinant wild type, indicates that the portion of the equation that is represented by k_{cat} (dissociation of the ES complex to form product) may be the limiting step, resulting in the overall low catalytic efficiency of the mutant enzymes (Table 11). The removal of the charged carboxylic acid group by the mutations D31Q, D31N and D31L and the introduction of additional hydrophobicity could have resulted in local perturbations and contributed to the differences observed in the CD spectra of these mutations (Figure 7).

The functionality of the mutant enzymes was also tested in vivo by assessing their ability to restore growth of a DHFR-deficient *E. coli*. This showed how severely dysfunctional these mutant enzymes were. Only the recombinant wild type and the control mutation V76A were able to restore growth of the *E. coli* DHFR deficient strain MG1655*folA::kan3* to levels comparable to its *E. coli* MG1655 parent strain in the absence of thymidine (Figure 10B). All of the D31 mutants were unable to complement

the missing DHFR gene of the deficient strain and subsequently no growth of the *E. coli* DHFR-deficient strain was observed when transformed with plasmid DNA that contained the *M. avium folA* gene with the respective mutation.

Therefore, one can conclude as hypothesized that aspartic acid 31 has an important functional role in catalysis in the *M. avium* DHFR. Replacing this residue with any other amino acid is certain to adversely affect efficient functionality of the enzyme. Both the charge of the aspartic acid as well as the spatial and geometric integrity of the binding cavity seem necessary for efficient functioning of the enzyme. While the enzyme may be able to accommodate local changes without effect on the overall three-dimensional structure of the enzyme, those changes, such as the replacement of conserved aspartic acid 31 in *M. avium* and structurally equivalent residues in other organisms could be fatal for the enzyme's normal and efficient functioning.

Functionality of *M. avium* conserved leucine 32 (L32) mutants

The L32 is one of several hydrophobic residues that line the enzyme's binding cavity, which is a common feature for all DHFRs described so far (14, 21, 29, 46, 47, 63). This residue is also conserved, but unlike D31 that was only substituted by glutamic acid in vertebrates, it is also replaced by glutamine in some bacteria, whereas vertebrates either have a phenylalanine or tyrosine in this position (47).

In this study L32 was substituted by phenylalanine (L32F), alanine (L32A) and aspartic acid (L32D). Human DHFR has phenylalanine in the equivalent position. One of the differences between bacterial and vertebrate DHFR is that vertebrate DHFRs are very resistant to trimethoprim, while bacterial DHFRs are very sensitive (5). Some studies (12,

47, 63) have looked at whether phenylalanine in this equivalent position in vertebrates plays a role in this difference.

In contrast to the D31 mutations, which all rendered the enzyme dysfunctional, only one of the 3 mutants of L32 caused a significant change in the enzyme's specific activity. The phenylalanine substitution (L32F), which is also hydrophobic, but much larger than the leucine residue of the recombinant wild type, did not cause a change in the enzyme's activity with the normal substrate as the percentage relative specific activity over the recombinant wild type shows (Table 12). The L32A mutation, which removed the hydrophobic side chain and is much smaller in size, also did not negatively impact the enzyme's normal function. This mutant still retained 96% of the specific activity of the recombinant wild type and was therefore statistically not different from the recombinant wild type enzyme (Tables 12 and 13). Only the L32D mutation affected the enzyme's normal reaction with the substrate dihydrofolate negatively. This mutant had only one third of the specific activity of the recombinant wild type enzyme and therefore was found to be statistically different from the recombinant wild type enzyme (Tables 12 and 13). These results indicate that unlike the D31 residue, L32 may not be directly involved in catalysis.

The catalytic behavior described before was also mirrored in the mutants' kinetic behavior. The $K_m(FAH_2)$ for the recombinant wild type, L32F and L32A were 0.7, 0.68 and 0.96 μM, respectively, and therefore, very similar to each other (Table 14). Only the L32D mutation had a 7-fold increase in $Km(FAH_2)$ over the recombinant wild type enzyme. Whereas the L32D mutation had a decrease in $k_{cat}(FAH_2)$ of only 3-fold over the recombinant wild type, the $k_{cat}/K_m(FAH_2)$ showed a 21-fold decrease (Table 14). The

L32F and L32A mutations also did not differ much from the recombinant wild type in k_{cat} and K_{cat}/K_m(FAH_2); for the L32F mutation this difference was less then 1 for both parameters, whereas they were 1.3 and 1.7, respectively, for the L32A mutation (Table 14). A similar study by Huang *et al.* (31), in which the equivalent L28 in *E. coli* DHFR was substituted by tyrosine (L28Y), found no changes in the Michaelis-Menten kinetics (K_m and k_{cat}) of the mutant compared to the recombinant wild type enzyme. Wagner *et al*. (65) compared the substitution of L28 in *E. coli* DHFR with phenylalanine (L28F) with the reciprocal mutation F31L in mouse DHFR, the equivalent position in vertebrate DHFR. The *E. coli* L28F mutant showed an increased k_{cat} (from 11 to 50 sec^{-1}), but the mutation had little effect on K_m(FAH_2). On the other hand, the F31L mutation in mouse DHFR showed a decreased k_{cat} (from 28 to 4.8 sec^{-1}), but also did not affect K_m(FAH_2). In both cases there was little affect on NADPH. This study did not observe the increase in k_{cat} for the L32F mutation in *M. avium* DHFR, that was found for the equivalent mutation in *E. coli* DHFR: however, similar to the L28F mutation in *E. coli* DHFR reported by Wagner *et al.*, k_{cat} and K_m(FAH_2) were not affected much in this study for the L32F mutation in *M. avium* DHFR (Table 14). The L32F mutation in *M. avium* DHFR also did not have an effect on the K_m(NADPH) (Table 14).

The data for the F31L mouse mutant reported by Wagner *et al*. (65) differ somewhat from Chunduru *et al*. (12) and Prendergast *et al*. (47), the two latter studies investigating the equivalent F31L mutation in human DHFR. Whereas Wagner *et al*. observed a decrease in k_{cat} and no effect on K_m, both Chunduru (12) and Prendergast (47), found sizeable increases in K_m(FAH_2); Prendergast (47), also found an almost 11-fold increase

in K_m(NADPH). Overall, this reciprocal mutation in vertebrates, led to a decrease in k_{cat}/k_m of the mutant (12, 47, 63, 65).

While this study did not find a change in the L32A mutant's activity compared to that of the recombinant wild type *M. avium* DHFR, Chunduru *et al.* (12) found that the equivalent mutant (F31A) in human DHFR had a 4-fold higher $K_m(FAH_2)$ and that k_{cat}/K_m was decreased by 4-fold. Nothing was found in the literature for the substitution of leucine in this position with aspartic acid. However, the introduction of a charged group with the aspartic acid substitution may have adverse effects on interactions in the binding cavity. Baccanari *et al.* (4) found 2 DHFR isozymes in *E. coli* (RT500) with the only difference between them being that one had leucine in position 28, whereas the other had arginine in position 28. They argued that interaction between this arginine in position 28 with the conserved aspartic acid in position 27, probably led to this mutants reduced efficiency. The CD spectra (Figure 7) show no difference between the recombinant wild type and the L32D mutation. It is therefore possible that the reduction in functionality of this mutation could be due to similar interactions in the binding cavity as described by Baccanari *et al.* (4), that led to the change in the mutants' catalytic and kinetic behavior. As previously discussed, X-ray crystal structures of *E. coli, L. casei* and DHFRs from other species reveal interactions of specific residues with substrate and inhibitors. On the basis of equivalencies (amino acid alignments), a functional interaction of L32 in *M. avium* with inhibitors was hypothesized. The L32 mutant enzymes were tested in an enzyme assay with trimethoprim, a widely used antibacterial agent, for which mycobacteria are naturally resistant. Bacterial DHFRs are highly sensitive to trimethoprim, whereas vertebrate DHFRs are not (47, 50). It is this characteristic that

makes trimethoprim a useful antibacterial agent. Two other deazapteridine antifolates were also tested for inhibitory effects against the recombinant wild type and L32 mutants. The results as IC_{50} values are listed in Table 15. The IC_{50} for trimethoprim of 3869 nM for the recombinant wild type compares well with the 4100 nM found the Suling *et al*. (58, 59) for *M. avium* DHFR. The L32F mutant was not very different from the recombinant wild type with an IC_{50} of 3647 nM for trimethoprim. Although the phenylalanine residue is much larger than the leucine of the wild type, this mutation did not negatively impact the hydrophobic nature of the area, suggesting that the enzyme is more flexible in this position. The reciprocal mutation in human DHFR (F31L) also did not affect that mutant enzyme's binding of trimethoprim compared to recombinant human DHFR (12, 47), which led Prendergast *et al.* (47) to conclude that the phenylalanine in that position in vertebrate DHFR does not account for the difference in vertebrate and bacterial DHFR with respect to trimethoprim binding. The L32A mutation's IC_{50} for *M. avium* DHFR in this study was increased about 12-fold over the recombinant wild type enzyme (Table 15). The L32A mutant removed the hydrophobic residue from this position which may have caused a change in local hydrophobicity. X-ray crystal structures have shown that the equivalent hydrophobic residue in *E. coli* and *L. casei* DHFRs are in contact with inhibitors. In their proposed model of the *M. avium* DHFR, Kharkar *et al.* (33) also point to the role of L32 in interacting with inhibitors. The current finding gives support for this role of L32 in *M. avium* DHFR. This decrease in selectivity to trimethoprim by the *M. avium* L32A mutant is also shown in the equivalent mutant (F31A) in human DHFR (12).

The L32D mutation in *M. avium* DHFR led to an almost 7-fold increase in selectivity of the mutant to trimethoprim, thereby increasing binding of trimethoprim over the recombinant wild type. Given the drastic decrease in normal enzyme function with the natural substrate described earlier for the L32D (Table 12) and the increased binding of trimethoprim by this mutant, the inhibitor has gained an advantage over the substrate in the mutant, whereas the substrate had the competitive advantage in the recombinant wild type enzyme. The introduction of the charge with the aspartic acid in the L32D mutation seems to interact or stabilize trimethoprim, but not the substrate dihydrofolate. In the known DHFR X-ray crystal structures of *L. casei* and *E. coli* the p-aminobenzoic acid ring of folate is closely aligned with L27 and L28, respectively (38, 39). Kharkar *et al.* (33) proposed the same for L32 in their model of the *M. avium* DHFR. The L32D mutation in *M. avium* DHFR did not only remove the hydrophobic residue that stabilized the folate, but introduced a charge that may destabilize folate in the binding cavity, thereby negatively affecting the folate activity. Structurally trimethoprim does not have the hydrophobic ring of folate, but protruding methoxy groups (Figure 2) that might interact with aspartic acid to stabilize the inhibitor.

Two 2,4-diamino-5-methyl-5-deazapteridines (SRI compounds 8858 and 20730) (Figure 3) that have previously been shown to be active against *M. avium*, (59) have also been tested against the L32 mutants of *M. avium* DHFR in comparison to the recombinant wild type. The IC_{50} values for these compounds are listed in Table 15. Compared to trimethoprim both compounds were highly active against the recombinant wild type DHFR enzyme. The IC_{50} for compound 8858 was 1.03 nM for the recombinant wild type, whereas for compound 20730 it was 1.96 nM. This represents an increase in selectivity of

over 3000 and almost 2000-fold, respectively. This study used the salt forms of the deazapteridines that were previously tested by Suling *et al.* (59) in the lipophilic form. The IC_{50} value of the lipophilic compound 8686 (salt form 8858) was 0.84 nM, and that of the lipophilic compound 20094 (salt form 20730) was 1.0 nM for the recombinant wild type *M. avium* DHFR. The IC_{50} values for compound 8858 tested in this study compares well with that obtained by Suling *et al.* (59) for the lipophilic form, while compound 20730 tested here was almost double the IC_{50} of the lipophilic form tested by Suling *et al.* (59) . The findings of this study are further support of the activity of these deazapteridine derivatives against *M. avium* DHFR.

All L32 mutants in this study showed increased selectivity compared to trimethoprim, further support the potency of these compounds for *M. avium* DHFR. However, compared to the recombinant wild type, there is a gradual decrease in selectivity in the mutants for both these compounds. This increase proceeds in the order L32F > L32D > L32A. Although there was no difference in IC_{50} between the recombinant wild type and the L32F mutant with respect to trimethoprim, there was almost a 15- and 20-fold difference in IC_{50} between the recombinant wild type the L32F mutant for the compounds 8858 and 20730, respectively (Table 15). Even though the phenylalanine in this position would not change the hydrophobic nature of the surroundings, its large size might be in too close contact with the substitutent groups R1 and R5 on the phenyl ring (Figure 3), thereby causing steric interference. The L32 side chain in the wild type enzyme is much smaller and may accommodate the substitutent groups on the phenyl ring of these compounds much better.

The L32D mutation of the *M. avium* DHFR showed an IC_{50} of 69 nM for compound 8858 and 134 nM for compound 20730. For compound 8858 this was about 8-fold lower than trimethoprim; compound 20730 was about 4-fold lower than trimethoprim. Nevertheless, both compounds 8858 and 20730 that were highly effective against the recombinant wild type enzyme, were now respectively 67-and 68-fold less effective in the L32D mutant of *M. avium* DHFR. As discussed earlier the trimethoprim seems to have been stabilized in the binding cavity by the charge group of the aspartic acid in the L32D mutation, but that was not the case for folate and it doesn't seem to be the case for the ether compounds 8858 or 20730. The position of the phenyl ring with substituents R1 and R5 in close proximity to the charge carboxylic acid in position 32, formally occupied by a smaller hydrophilic residue, could also lead to steric interferences and affect binding of these compounds.

The last mutation in this series, L32A, that was highly insensitive against trimethoprim with an IC_{50} of 45067 nM, had an IC_{50} of 507 nM for compound 8858 and 861 nM for compound 20730. Despite the fact that the L32A mutation of *M. avium* DHFR seems to have had an increased sensitivity for the SRI compounds over trimethoprim, the difference between this mutation and the recombinant wild type was only about 12-fold for trimethoprim, but it was 492-fold for compound 8858 and 439-fold for compound 20730. In addition to removing the hydrophobic side chain of L32 present in the wild type, the alanine residue in the L32A mutant has the smallest side chain of all the mutants tested. Therefore there is little opportunity for either interference or interaction with the SRI compounds. The favorable interaction and stabilizing effect of the hydrophobic L32

residue is absent in the L32A mutant and therefore the large difference in IC_{50} between the recombinant wild type and the L32A mutants for both compounds 8858 and 20730. In summary the hypothesis, that was based on previous findings in *E. coli, L. casei* and DHFR's of other species, that L32 in *M. avium* DHFR plays a functional role in the binding of antifolates such as trimethoprim and the 2,4- diaminodeazapteridines described earlier and tested in this study, was supported by the findings of this study. However, unlike D31 in *M. avium* DHFR, L32 substitution by another hydrophobic residue (L32F) did not affect the enzymes normal function, even though phenylalanine is larger than the wild type leucine residue in position 32. This indicates that leucine may not play a role or not a direct role in catalysis. The rather high reduction in enzyme function by the L32D mutation could therefore be as a result of secondary factors. This substituted aspartic acid may interact with the residue D31, which has been shown in this study and in others to affect enzyme functionality.

CHAPTER V

CONCLUSION

The finding of this study for *M. avium* DHFR is consistent with what is currently known about the highly conserved binding cavity aspartic acid residue in *E. coli, L. casei* and other DHFR's. Aspartic acid 31 in *M. avium* DHFR plays a functional role in catalysis. Modification of size and charge (D31A, D31E and D31Q) and charge (D31N and D31L) resulted in a significant reduction of normal enzyme activity.

The findings of this study also support the hypothesis that L32 plays a functional role in the binding of antifolate inhibitors such as trimethoprim and 2,4-deazapteridines. It has been shown that modification of L32 in *M. avium* DHFR (L32D) made the enzyme more sensitive to trimethoprim, a current drug for which the organism is naturally resistant. It has also been shown that modifications of L32 in *M. avium* DHFR (L32A and L32D) have decreased selectivity of the enzyme for current potential inhibitors such as the 2,4-diaminodeazapteridines.

REFERENCES

1. **Adams, J., K. Johnson, R. Matthews, and S. J. Benkovic.** 1989. Effects of distal point-site mutations on the binding and catalysis of dihydrofolate reductase from Escherichia coli. Biochemistry **28:**6611-8.

2. **Appleman, J. R., E. E. Howell, J. Kraut, and R. L. Blakley.** 1990. Role of aspartate 27 of dihydrofolate reductase from Escherichia coli in interconversion of active and inactive enzyme conformers and binding of NADPH. J Biol Chem **265:**5579-84.

3. **Appleman, J. R., E. E. Howell, J. Kraut, M. Kuhl, and R. L. Blakley.** 1988. Role of aspartate 27 in the binding of methotrexate to dihydrofolate reductase from Escherichia coli. J Biol Chem **263:**9187-98.

4. **Baccanari, D. P., D. Stone, and L. Kuyper.** 1981. Effect of a single amino acid substitution on Escherichia coli dihydrofolate reductase catalysis and ligand binding. J Biol Chem **256:**1738-47.

5. **Baker, D. J., C. R. Beddell, J. N. Champness, P. J. Goodford, F. E. Norrington, D. R. Smith, and D. K. Stammers.** 1981. The binding of trimethoprim to bacterial dihydrofolate reductase. FEBS Lett **126:**49-52.

6. **Basran, J., M. G. Casarotto, I. L. Barsukov, and G. C. Roberts.** 1995. Role of the active-site carboxylate in dihydrofolate reductase: kinetic and spectroscopic studies of the aspartate 26-->asparagine mutant of the Lactobacillus casei enzyme. Biochemistry **34:**2872-82.

7. **Birdsall, B., J. Andrews, G. Ostler, S. J. Tendler, J. Feeney, G. C. Roberts, R. W. Davies, and H. T. Cheung.** 1989. NMR studies of differences in the conformations and dynamics of ligand complexes formed with mutant dihydrofolate reductases. Biochemistry **28:**1353-62.

8. **Bitar, K. G., D. T. Blankenship, K. A. Walsh, R. B. Dunlap, A. V. Reddy, and J. H. Freisheim.** 1977. Amino acid sequence of dihydrofolate reductase from an amethopterin-resistant strain of Lactobacillus casei. FEBS Lett **80:**119-22.

9. **Bleyer, W. A.** 1978. The clinical pharmacology of methotrexate. New applications of an old drug. Cancer Treat. Rev. **41:**36-51.

10. **Bystroff, C., S. J. Oatley, and J. Kraut.** 1990. Crystal structures of Escherichia coli dihydrofolate reductase: the NADP+ holoenzyme and the folate.NADP+ ternary complex. Substrate binding and a model for the transition state. Biochemistry **29:**3263-77.

11. **Chen, J. T., R. J. Mayer, C. A. Fierke, and S. J. Benkovic.** 1985. Site-specific mutagenesis of dihydrofolate reductase from Escherichia coli. J Cell Biochem **29:**73-82.

12. **Chunduru, S. K., V. Cody, J. R. Luft, W. Pangborn, J. R. Appleman, and R. L. Blakley.** 1994. Methotrexate-resistant variants of human dihydrofolate reductase. Effects of Phe31 substitutions. J Biol Chem **269:**9547-55.

13. **Cody, V., N. Galitsky, D. Rak, J. R. Luft, W. Pangborn, and S. F. Queener.** 1999. Ligand-induced conformational changes in the crystal structures of Pneumocystis carinii dihydrofolate reductase complexes with folate and NADP+. Biochemistry **38:**4303-12.

14. **Cody, V., J. R. Luft, and W. Pangborn.** 2005. Understanding the role of Leu22 variants in methotrexate resistance: comparison of wild-type and Leu22Arg variant mouse and human dihydrofolate reductase ternary crystal complexes with methotrexate and NADPH. Acta Crystallogr D Biol Crystallogr **61:**147-55.

15. **Czaplinski, K.-H., W. Hänsel, M. Wiese, and J. K. Seydel.** 1995. New benzylpyrimidines: inhibition of DHFR from various species. QSAR, CoMFA and PC analysis. Eur. J. Med. Chem. **30:**779-787.

16. **Dale, G. E., C. Broger, A. D'Arcy, P. G. Hartman, R. DeHoogt, S. Jolidon, I. Kompis, A. M. Labhardt, H. Langen, H. Locher, M. G. Page, D. Stuber, R. L. Then, B. Wipf, and C. Oefner.** 1997. A single amino acid substitution in Staphylococcus aureus dihydrofolate reductase determines trimethoprim resistance. J Mol Biol **266:**23-30.

17. **Dale, G. E., H. Langen, M. G. Page, R. L. Then, and D. Stuber.** 1995. Cloning and characterization of a novel, plasmid-encoded trimethoprim-resistant dihydrofolate reductase from Staphylococcus haemolyticus MUR313. Antimicrob Agents Chemother **39:**1920-4.

18. **David, C. L., E. E. Howell, M. F. Farnum, J. E. Villafranca, S. J. Oatley, and J. Kraut.** 1992. Structure and function of alternative proton-relay mutants of dihydrofolate reductase. Biochemistry **31:**9813-22.

19. **Dunn, S. M., T. M. Lanigan, and E. E. Howell.** 1990. Dihydrofolate reductase from Escherichia coli: probing the role of aspartate-27 and phenylalanine-137 in enzyme conformation and the binding of NADPH. Biochemistry **29:**8569-76.

20. **Ellner, J. J., M. J. Goldberger, and D. M. Parenti.** 1991. *Mycobacterium avium* infection and AIDS: A therapeutic dilemma in rapid evolution. J. Infect. Dis. **163:**1326-1335.

21. **Falzone, C. J., P. E. Wright, and S. J. Benkovic.** 1991. Evidence for two interconverting protein isomers in the methotrexate complex of dihydrofolate reductase from Escherichia coli. Biochemistry **30:**2184-91.

22. **Fierke, C. A., and S. J. Benkovic.** 1989. Probing the functional role of threonine-113 of Escherichia coli dihydrofolate reductase for its effect on turnover efficiency, catalysis, and binding. Biochemistry **28:**478-86.

23. **Ghassemi, M., B. R. Andersen, V. M. Reddy, P. R. Gangadharam, G. T. Spear, and R. M. Novak.** 1995. Human immunodeficiency virus and *Mycobacterium avium* complex coinfection of monocytoid cells results in reciprocal enhancement of multiplication. J Infect Dis. **171:**68-73.

24. **Hartman, P. G.** 1993. Molecular aspects and mechanism of action of dihydrofolate reductase inhibitors. J. Chemother. **5:**369-376.

25. **Herrington, M. B., and N. T. Chirwa.** 1999. Growth properties of a folA null mutant of *Escherichia coli* K12. Can. J. Microbiol. **45:**191-200.

26. **Hillcoat, B. L., P. F. Dixon, and R. L. Blakley.** 1967. Effect of substrate decomposition on the spectrophotometric assay of dihydrofolate reductase. Anal. Biochem. **21:**178-189.

27. **Hitchings, G. H. J.** 1989. Nobel lecture in physiology or medicine-1988. Selective inhibitors of dihydrofolate reductase. In Vitro Cell. Dev. Biol. **25:**303-310.

28. **Horsburgh, C. R.** 1991. Mycobacterium avium complex infection in the acquired immunodifficiency syndrome. N. Engl. J. Med. **324:**1332-1338.

29. **Howell, E. E., C. Booth, M. Farnum, J. Kraut, and M. S. Warren.** 1990. A second-site mutation at phenylalanine-137 that increases catalytic efficiency in the mutant aspartate-27----serine Escherichia coli dihydrofolate reductase. Biochemistry **29:**8561-9.

30. **Howell, E. E., J. E. Villafranca, M. S. Warren, S. J. Oatley, and J. Kraut.** 1986. Functional Role of Aspartic Acid-27 in Dihydrofolate Reductase Revealed by Muragenesis. Science **231:**1123-1128.

31. **Huang, Z., C. R. Wagner, and S. J. Benkovic.** 1994. Nonadditivity of mutational effects at the folate binding site of Escherichia coli dihydrofolate reductase. Biochemistry **33:**11576-85.

32. **Kansy, M., J. K. Seydel, M. Wiese, and R. Haller.** 1992. Synthesis of new 2,4-diamino-5-benzylpyrimidines active against various bacterial species. Eur. J. Med. Chem. **27:**237-244.

33. **Kharkar, P., and V. M. Kulkarni.** 2003. A proposed model of Mycobacterium avium complex dihydrofolate reductase and its utility for drug design. Org. Biomol. Chem. **1:**1315-1322.

34. **Li, L. Y., and S. J. Benkovic.** 1991. Impact on catalysis of secondary structural manipulation of the alpha C-helix of Escherichia coli dihydrofolate reductase. Biochemistry **30:**1470-8.

35. **Li, R., R. Sirawaraporn, P. Chitnumsub, W. Sirawaraporn, J. Wooden, F. Athappilly, S. Turley, and W. G. Hol.** 2000. Three-dimensional structure of M. tuberculosis dihydrofolate reductase reveals opportunities for the design of novel tuberculosis drugs. J Mol Biol **295:**307-23.

36. **Locher, H. H., H. Schlunegger, P. G. Hartman, P. Angehrn, and R. L. Then.** 1996. Antibacterial activities of epiroprim, a new dihydrofolate reductase inhibitor, alone and in combination with dapsone. Antimicrob. Agents Chemother. **40:**1376-1381.

37. **Masters, J. N., and G. Attardi.** 1983. The nucleotide sequence of the cDNA coding for the human dihydrofolic acid reductase. Gene **21:**59-63.

38. **Matthews, D. A., R. A. Alden, J. T. Bolin, D. J. Filman, S. T. Freer, R. Hamlin, W. G. Hol, R. L. Kisliuk, E. J. Pastore, L. T. Plante, N. Xuong, and J. Kraut.** 1978. Dihydrofolate reductase from Lactobacillus casei. X-ray structure of the enzyme methotrexate.NADPH complex. J Biol Chem **253:**6946-54.

39. **Matthews, D. A., R. A. Alden, J. T. Bolin, S. T. Freer, R. Hamlin, N. Xuong, J. Kraut, M. Poe, M. Williams, and K. Hoogsteen.** 1977. Dihydrofolate reductase: x-ray structure of the binary complex with methotrexate. Science **197:**452-5.

40. **Mayer, R. J., J. T. Chen, K. Taira, C. A. Fierke, and S. J. Benkovic.** 1986. Importance of a hydrophobic residue in binding and catalysis by dihydrofolate reductase. Proc Natl Acad Sci U S A **83:**7718-20.

41. **McCourt, M., and V. Cody.** 1991. Conformational analysis of lipophilic antifolates: Crystal structure of 2-amino-4-oxo-6-adamantylpteridine and a comparison of its binding to bacterial and avian dihydrofolate reductase. J. Am. Chem. Soc. **113:**6634-6639.

42. **Meyer, S. C. C., S. K. Majumder, and M. H. Cynamon.** 1995. In vitro activities of PS-15, a new dihydrofolate reductase inhibitor, and its cyclic metabolite against *Mycobacterium avium* complex. Antimicrob. Agents Chemother. **39:**1862-1863.

43. **Morris, S. L., and D. A. Rouse.** 1996. The genetics of multiple drug resistance in *Mycobacterium tuberculosis* and the *Mycobacterium avium* Complex. Res. Microbiol. **147:**68-73.

44. **Murphy, D. J., and S. J. Benkovic.** 1989. Hydrophobic interactions via mutants of Escherichia coli dihydrofolate reductase: separation of binding and catalysis. Biochemistry **28:**3025-31.

45. **Oefner, C., A. D'Arcy, and F. K. Winkler.** 1988. Crystal structure of human dihydrofolate reductase complexed with folate. Eur. J. Biochem. **174:**377-85.

46. **Polshakov, V. I.** 2001. Dihydrofolate reductase: structural aspects of mechanisms of enzyme catalysis and inhibition. Russian Chemical Bulletin, International Edition **50:**1733-1751.

47. **Prendergast, N. J., J. R. Appleman, T. J. Delcamp, R. L. Blakley, and J. H. Freisheim.** 1989. Effects of conversion of phenylalanine-31 to leucine on the function of human dihydrofolate reductase. Biochemistry **28:**4645-50.

48. **Prendergast, N. J., T. J. Delcamp, P. L. Smith, and J. H. Freisheim.** 1988. Expression and site-directed mutagenesis of human dihydrofolate reductase. Biochem. **27:**3664-3671.

49. **Reddy, V. M.** 1998. Mechanism of Mycobacterium avium complex pathogenesis. Front. Biosci. **3:**525-531.

50. **Rosowsky, A., R. A. Forsch, and S. F. Queener.** 1995. 2,4-Diaminopyrido[3,2-d]pyrimidine inhibitors of dihydrofolate reductase from Pneumocystis carinii and Toxoplasma gondii. J Med Chem **38:**2615-20.

51. **Rouch, D. A., L. J. Messerotti, L. S. Loo, C. A. Jackson, and R. A. Skurray.** 1989. Trimethoprim resistance transposon Tn4003 from Staphylococcus aureus encodes genes for a dihydrofolate reductase and thymidylate synthetase flanked by three copies of IS257. Mol Microbiol **3:**161-75.

52. **Saxena, A. K., and M. Saxena.** 1986. Advances in chemotherapy of malaria. Prog. Drug Res. **30:**221-280.

53. **Schweitzer, B. I., A. P. Dicker, and J. R. Bertino.** 1990. Dihydrofolate reductase as a therapeutic target. FASEB **4:**2441-2452.

54. **Shortel, D., D. DiMaio, and D. Nathans.** 1981. Directed Mutagenesis. Ann. Rev. Genet. **15:**265-294.

55. **Snider, D. E., and J. R. La Montagne.** 1994. The neglected global tuberculosis problem: a report of the 1992 World Congress on Tuberculosis. J. Infect. Dis. **169:**1189-1196.

56. **Sreerama, N., S. Y. Venyaminov, and R. W. Woody.** 2000. Estimation of protein secondary structure from circular dichroism spectra: inclusion of denatured proteins with native proteins in the analysis. Anal Biochem **287:**243-51.

57. **Stone, S. R., and J. F. Morrison.** 1984. Catalytic mechanism of the dihydrofolate reductase reaction as determined by pH studies. Biochemistry **23:**2753-8.

58. **Suling, W. J., R. C. Reynolds, E. W. Barrow, L. N. Wilson, J. R. Piper, and W. W. Barrow.** 1998. Susceptibilities of *Mycobacterium tuberculosis* and *Mycobacterium avium* complex to lipophilic deazapteridine derivatives, inhibitors of dihydrofolate reductase. J. Antimicrob. Chemotherapy **42:**811-815.

59. **Suling, W. J., L. E. Seitz, V. Pathak, L. Westbrook, E. W. Barrow, S. Zywno-van Ginkel, R. C. Reynolds, J. R. Piper, and W. W. Barrow.** 2000. Antimycobacterial Activities of 2,4-Diamino-5-Deazapteridine Derivatives and Effects on Mycobacterial Dihydrofolate Reductase. Antimicrobial Agents and Chemotherapy **44:**2784-2793.

60. **Taira, K., and S. J. Benkovic.** 1988. Evaluation of the importance of hydrophobic interactions in drug binding to dihydrofolate reductase. J Med Chem **31:**129-37.

61. **Thillet, J., J. Absil, S. R. Stone, and R. Pictet.** 1988. Site-directed mutagenesis of mouse dihydrofolate reductase. Mutants with increased resistance to methotrexate and trimethoprim. J Biol Chem **263:**12500-8.

62. **Thillet, J., J. A. Adams, and S. J. Benkovic.** 1990. The kinetic mechanism of wild-type and mutant mouse dihydrofolate reductases. Biochemistry **29:**5195-202.

63. **Tsay, J. T., J. R. Appleman, W. A. Beard, N. J. Prendergast, T. J. Delcamp, J. H. Freisheim, and R. L. Blakley.** 1990. Kinetic investigation of the functional role of phenylalanine-31 of recombinant human dihydrofolate reductase. Biochemistry **29:**6428-36.

64. **Villafranca, J. E., E. E. Howell, D. H. Voet, M. S. Strobel, R. C. Ogden, J. N. Abelson, and J. Kraut.** 1983. Directed Mutagenesis of Dihydrofolate Reductase. Science **222:**782-788.

65. **Wagner, C. R., J. Thillet, and S. J. Benkovic.** 1992. Complementary perturbation of the kinetic mechanism and catalytic effectiveness of dihydrofolate reductase by side-chain interchange. Biochemistry **31:**7834-40.

66. **Warren, M. S., K. A. Brown, M. F. Farnum, E. E. Howell, and J. Kraut.** 1991. Investigation of the Functional Role of Tryptophan-22 in *Escherichia coli* Dihydrofolate Reductase by Site-directed Mutagenesis. Biochemistry **30:**11092-11103.

67. **Wyss, P. C., P. Gerber, P. G. Hartman, C. Hubschwerlen, H. Locher, H. P. Marty, and M. Stahl.** 2003. Novel dihydrofolate reductase inhibitors. Structure-based versus diversity-based library design and high-throughput synthesis and screening. J Med Chem **46:**2304-12.

68. **Zoller, M. J., and M. Smith** 1982. Oligonucleotide-directed mutagenesis using M13-derived vectors: an efficient and general procedure for the production of point mutations in any fragment of DNA. Nucleic Acid Research **10:**6487-6500.

69. **Zywno-van Ginkel, S., T. P. Dooley, W. J. Suling, and W. W. Barrow.** 1997. Identification and cloning of the *Mycobacterium avium fol*A gene, required for dihydrofolate reductase activity. FEM Microbiology Letters **156:**69-78.

VITA

RONNIE A. BOCK

Candidate for the Degree of

Doctor of Philosophy

Thesis: FUNCTIONAL ROLE OF ASPARTATE-31 AND LEUCINE-32 IN *MYCOBACTERIUM AVIUM* DIHYDROFOLATE REDUCTASE

Major Field: Veterinary Biomedical Science

Biographical:

Personal Data: Born in Namibia, June 11, 1962.
Education: Graduated from Universität des Saarlandes (Germany) in Biology (1996). Completed the requirements for the Doctor of Philosophy degree at the Oklahoma State University in May, 2006.
Experience: Veterinary Technician, Veterinary Services**,** Ministry of Agriculture, Government of Namibia. Lecturer: Department of Biology at the University of Namibia
Professional Memberships: American Society for Microbiology, Namibian Biotechnology Alliance

Name: Ronnie A. Bock Date of Degree: May, 2006

Institution: Oklahoma State University Location: Stillwater, Oklahoma

Title of Study: FUNCTIONAL ROLE OF ASPARTATE-31 AND LEUCINE-32 IN *MYCOBACTERIUM AVIUM* DIHYDROFOLATE REDUCTASE

Pages in Study: 100 Candidate for the Degree of Doctor of Philosophy

Major Field: Veterinary Biomedical Science

Scope and Method of Study:
Dihydrofolate reductase (DHFR: 1.5.1.3) has long been a drug target in antibacterial therapy. However, DHFR of *Mycobacterium avium* and other mycobacteria are naturally resistant to trimethoprim and other antituberculous drugs. Recent reports show that a new class of drugs: 2,4-diaminodeazapteridine (DMDPs) are showing increased selectivity for *Mycobacterium avium*. Better understanding of the binding sites of *M. avium* DHFR, will contribute towards developing better and more effective drugs.Based on sequence alignments and X-ray crystal structures of other DHFR's, aspartic acid 31 (D31) and leucine 32 (L32) were identified as functionally important residues in interactions with the substrate dihydrofolate and inhibitors, respectively. D31 and L32 of *M. avium* DHFR were modified by site-directed mutagenesis (GeneEditor, Promega). to D31A, D31E, D31Q, D31N, D31L,. L32A, L32F and L32D. Mutations were verified by full length gene sequencing. These mutants were then expressed in *E. coli* BL21(DE3)pLysS and the recombinant mutant protein purified using HisBind-Resin (Novangen). Functionality of the mutants was assessed in comparison with the recombinant wild type by a standard enzyme assay as well as by growth complementation. Kinetic parameters were determined and computed using the non-linear curve fit program Enzfitter (BioSoft, UK).

Findings and Conclusions:
All D31 mutations rendered the enzyme severely dysfunctional. Enzyme activity of he mutants D31E, D31Q and D31N were reduced by between 80 and 90%. Functionality of the mutants D31A and D31L were reduced by over 90% compared to the wild type.

All D31 mutants show differences in kinetics compared to the wild type. Of the L32 mutants, only L32D reduced the enzyme's activity by two-thirds and showed differences in kinectic behavior compared to the wild type. L32F and L32A did not show selectivity for trimethoprim, while L32D did. The DMDP inhibitors were highly effective against the wild type. The mutatants showed differences in selectivity to the DMDPs.
The findings support the hypostheses that D31 plays a functional role with the substrate and L32 plays a functional role with inhibitors. All D31 mutations studies resulted in a dysfunctional enzyme, regardless of changes in side chain size or charge. Modification of L32 led to increased selectivity for trimethoprim, but decreased selectivity for the DMDPs.

ADVISER'S APPROVAL: Dr. W. W. Barrow